~~CONFIDENTIAL~~

OFFICE OF SCIENTIFIC RESEARCH & DEVELOPMENT

NATIONAL DEFENSE RESEARCH COMMITTEE.

DIVISION SIX-SECTION 6.1

MEASUREMENTS OF THE

HIGH FREQUENCY NOISE PRODUCED BY CAVITATING PROJECTILES

IN THE

HIGH SPEED WATER TUNNEL

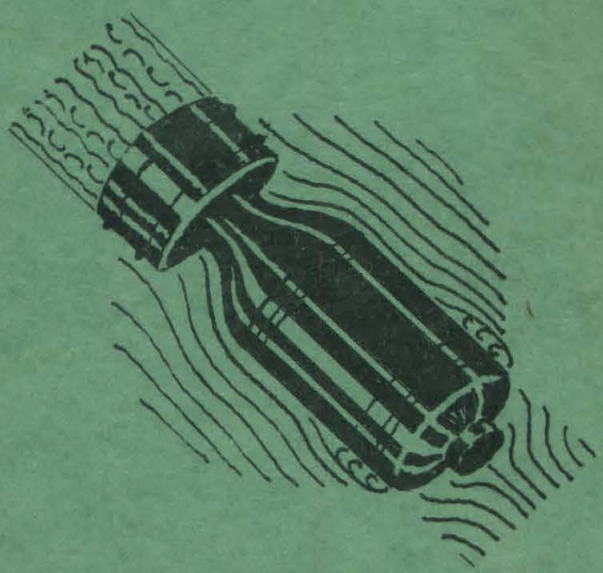

THE HIGH SPEED WATER TUNNEL
CALIFORNIA INSTITUTE OF TECHNOLOGY
PASADENA, CALIFORNIA.

SECTION Nº 6.1-Sr-207-924

COPY Nº 2

FILE COPY

(CONFIDENTIAL)

OFFICE OF SCIENTIFIC RESEARCH AND DEVELOPMENT
NATIONAL DEFENSE RESEARCH COMMITTEE
DIVISION SIX – SECTION 6.1

MEASUREMENTS OF THE HIGH FREQUENCY NOISE PRODUCED BY CAVITATING PROJECTILES IN THE HIGH SPEED WATER TUNNEL

BY

ROBERT T. KNAPP
OFFICIAL INVESTIGATOR

THE HIGH SPEED WATER TUNNEL
AT THE
CALIFORNIA INSTITUTE OF TECHNOLOGY
HYDRAULIC MACHINERY LABORATORY
PASADENA, CALIFORNIA

Section No. 6.1-sr-207-924
HML Rep. No. ND-8.2

August 31, 1943

TABLE OF CONTENTS

REPORT

Section No.		Page No.
I.	PURPOSE OF INVESTIGATION	2
II.	DESCRIPTION OF TEST INSTALLATION	2
III.	DESCRIPTION OF OPERATING PROCEDURE AND METHOD OF PRESENTING RESULTS	3
IV.	TUNNEL BACKGROUND NOISE	7
V.	THE VARIATION OF SOUND INTENSITY WITH THE BEGINNING AND GROWTH OF CAVITATION	12
VI.	FREQUENCY DISTRIBUTION MEASUREMENTS — EFFECT OF RELATIVE POSITION OF HYDROPHONE AND MODEL	28
VII.	THE EFFECT OF VELOCITY ON THE MEASURED SOUND INTENSITY	34

APPENDIX

I.	DESCRIPTION OF SOUND MEASURING EQUIPMENT	37
II.	OPERATION OF SOUND MEASURING EQUIPMENT	39
III.	CALIBRATION OF EQUIPMENT AND CALCULATION OF RESULTS	39
IV.	HYDRAULIC PRESSURE CONTROL SYSTEM	40
V.	REFERENCES	Following Appendix Figures

ABSTRACT

The High Speed Water Tunnel is operated by the California Institute of Technology under Contract OEMsr-207 and is sponsored by Division 6, Section 6.1 of the NDRC of the OSRD. The experiments reported in this memorandum were requested by the office of the Chief of Section 6.1.

The report presents the results of preliminary measurements of the sound produced in the 20 to 100 kilocycle frequency range by cavitating projectiles in the Water Tunnel working section. Measurements were made of the noise intensity in the 20-100 kilocycle frequency band with three different projectiles. Measurements of the intensity and distribution of the noise within this band were made with one of these projectiles.

The main findings regarding the production and measurement of the sound are:

(1) Sound intensity increases sharply as cavitation appears visibly to several times the magnitude of any noise measured under non-cavitating conditions.

(2) The measured intensity falls off as cavitation at a given zone develops but with the start of cavitation at any new point, the intensity rises abruptly again.

(3) Conclusions (1) and (2) are valid for cavitation at pressures above or below atmospheric.

(4) The intensity of the noise produced by cavitation increases with the velocity. In the range of frequencies and velocities investigated, the rate of sound intensity increase is proportional to at least the first power of velocity.

(5) The frequency distribution of the sound produced by cavitation depends on both the pressure and the velocity at which the cavitation occurs.

(6) Measurements leading to these conclusions are possible because the components of the sound generated by the Tunnel itself in the range above 20 kilocycles are small compared to the noise produced by cavitation on the projectile.

In addition, with respect to the particular models tested it was found that:

(1) By streamlining the nose of the projectile, the onset of cavitation at the nose and the resulting production of sound can be delayed to lower pressures for constant velocity operation or to higher velocities for constant pressure (submergence) operation.

(2) As the projectile yaws, cavitation occurs at a higher pressure or lower velocity for both nose and tail structure.

(3) At an angle of yaw the benefits of a streamlined nose may vanish, since cavitation on the tail structure and the resulting production of noise occur at a higher pressure ~~of~~ OR lower velocity than does cavitation on the nose.

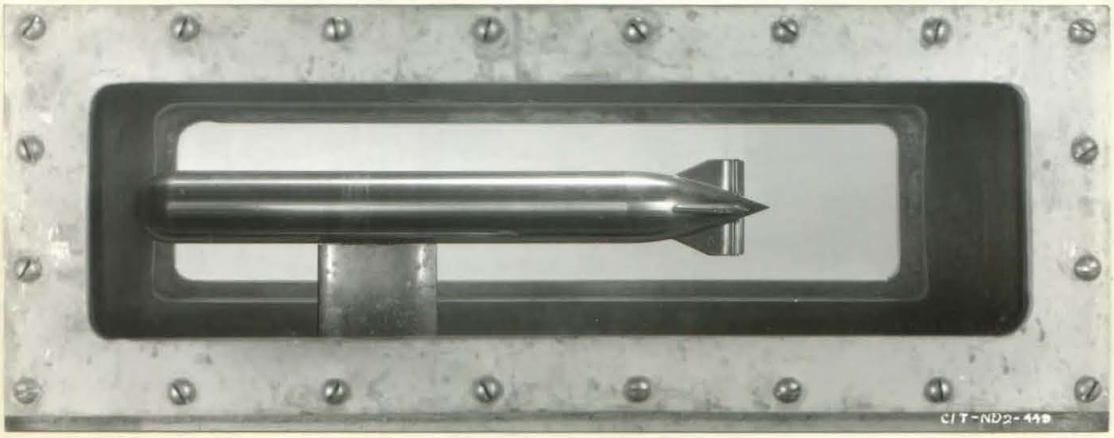

FIGURE 1

2" DIAMETER MODEL PROJECTILE
SHOWN MOUNTED IN 14" DIAMETER WORKING SECTION
OF THE HIGH SPEED WATER TUNNEL

MEASUREMENTS OF THE HIGH FREQUENCY NOISE PRODUCED BY CAVITATING PROJECTILES IN THE HIGH SPEED WATER TUNNEL

I. PURPOSE OF INVESTIGATION

This report presents the results of a preliminary investigation of the high frequency sound caused by the flow around projectiles in a high velocity stream of water. The purpose of this investigation was to determine the magnitude and distribution of the high frequency components of the noise produced as cavitation begins and as the cavitating zone grows. The measurements were made in the High Speed Water Tunnel at the California Institute of Technology with special equipment designed to measure and analyze the sound in the frequency range of 1 to 100 kilocycles.

II. DESCRIPTION OF TEST INSTALLATION

The sound studies were made with 2" diameter model projectiles mounted in the 14" diameter working section of the High Speed Water Tunnel.(1) Figure 1 shows a model supported from the bottom of the working section by a streamline strut. In this photograph both the model and the strut are aligned with the axis of the working section so as to be parallel to the flow. The installation is arranged, however, so the model can be yawed with respect to the flow while the strut alignment remains unchanged. A special profile shape for the strut tends to prevent cavitation on the strut surface except at very low pressures or very high velocities.

The hydrophone used to detect the sounds coming from the flow around the model was mounted in a water filled lucite "blister", clamped against one of the lucite side windows of the tunnel working section. Provision was made for moving the hydrophone to various positions. Figure 2 shows a photograph of the hydrophone mounted for use and Figure 3 shows the details of the hydrophone and the lucite mounting blister. Rubber grommets were used to isolate the hydrophone unit in order to minimize the transmission of mechanical vibrations to it. This exterior type of mounting was adopted because, first, it was not feasible to put the instrument inside the models being used, and second, it was desirable to eliminate the possibility of extraneous noise from flow around a submerged hydrophone housing. It has been found by other laboratories working with sound equipment that in the transmission of sound, lucite behaves similarly to water. Consequently, it was expected that no appreciable error would result from reflections at the interface between the lucite and the water.

The sound measuring equipment was designed to amplify the output of the detecting hydrophone in selected frequency ranges and to indicate the amplified voltage on a meter. The actual sound intensity in dynes per square centimeter is proportional

(1) **Figures refer to references listed at the end of this report.**

to the voltage recorded.# A block diagram of the sound detecting and measuring apparatus is shown in Figure 4. A complete description of the apparatus and its characteristics will be found in the appendix to this report.

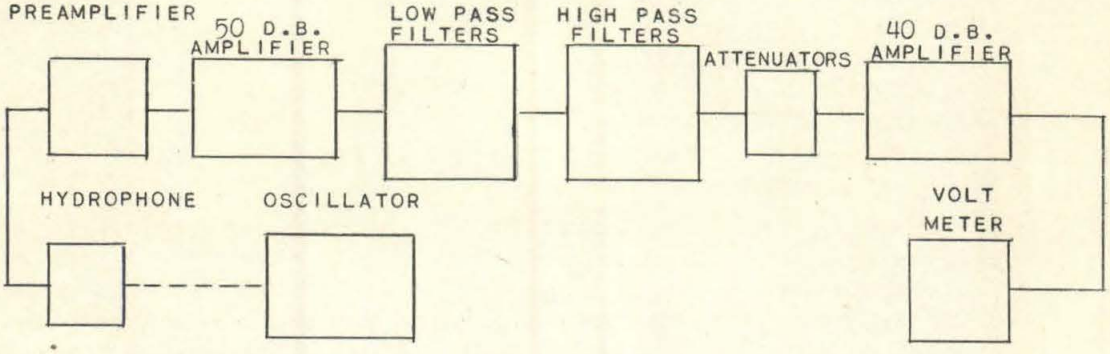

FIGURE 4

BLOCK DIAGRAM OF SOUND DETECTING AND MEASURING EQUIPMENT

III. DESCRIPTION OF OPERATING PROCEDURE AND METHOD OF PRESENTING RESULTS

In the operation of the Water Tunnel there are two methods of causing cavitation to develop on the models. One is to maintain a fixed pressure in the working section and to increase the water velocity. This corresponds to studying the behavior of the projectile running at a constant depth of submergence. The other method is to maintain a constant velocity and to vary the pressure in the working section. This, of course, corresponds to variable submergence, constant speed operation. Within certain limitations discussed in this report, the data obtained by either method can be used to predict the entire behavior of the projectile. The latter method offers an important advantage for Water Tunnel tests because the control equipment is such that while the velocity cannot be adjusted independently of the pressure, the pressure can be changed independently of the velocity* Consequently, all tests were made using this procedure.

Three simultaneous quantities are measured during the sound surveys. They are the intensity of sound in dynes per square centimeter, the velocity of flow past the projectile in feet per second (V), and the pressure in the working section in pounds per

As described in the Appendix the hydrophone actually is sensitive to the *acoustic pressure* and the output voltage is proportional to this pressure measured in dynes per square centimeter. The term "sound intensity" has been used throughout this report instead of acoustic pressure so as to distinguish clearly between the hydraulic pressure and the acoustic pressure.

* See the appendix of this report and reference (1) for a description of the speed control and pressure regulation systems.

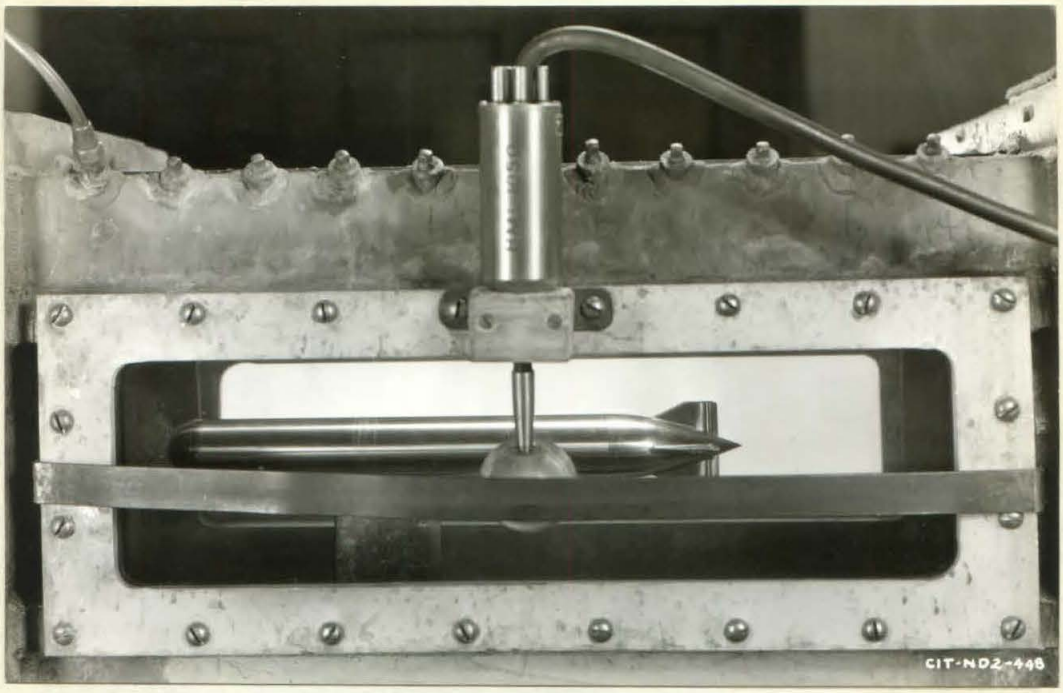

FIGURE 2

BRUSH HYDROPHONE
MOUNTED ON LUCITE WINDOW OF WORKING SECTION

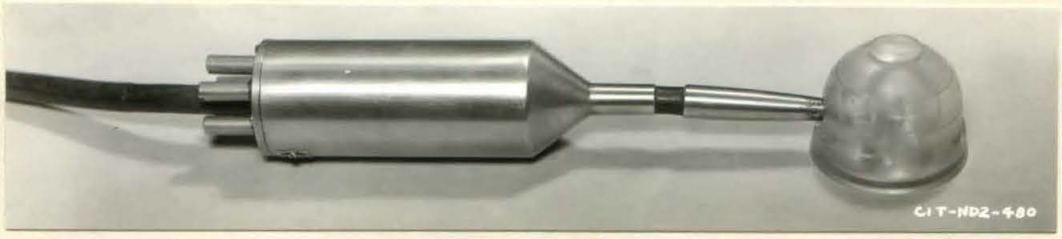

FIGURES 3A AND 3B

DETAILS OF HYDROPHONE AND LUCITE MOUNTING BLISTER

square inch (P/144). The sound is detected by the hydrophone mounted on the Water Tunnel working section window as described in Section II. The magnitude of the measured intensity is approximately proportional to the root-mean-square value of all components within the selected frequency band. The hydraulic pressure is taken from any one of a series of pressure taps in the working section wall. The values of pressure used in presenting the results are all referred to a point opposite the projectile nose. The velocity is obtained from measurements of the pressure drop across the nozzle at the entrance to the working section.

According to the usual conception, cavitation occurs when the absolute pressure at some point in the flow drops to the vapor pressure (P_v) of the liquid. Consequently, for a given velocity it is the margin between the absolute pressure in the main flow and the vapor pressure ($P-P_v$) that indicates whether or not cavitation will occur. If the velocity is variable, however, ($P-P_v$) is not sufficient to indicate the tendency for cavitation to begin. For an object in a fluid stream there are local pressures on its surfact that are less than the pressure of the main flow. This local pressure reduction is affected by the velocity; in fact, it is proportional to the dynamic pressure of the main stream. The dynamic pressure is $\rho \frac{v^2}{2}$ where ρ is the density of the fluid in slugs per cubic foot. If either the flow velocity is increased or the pressure of the main stream is reduced, the local pressure may be reduced to the vapor pressures of the liquid causing cavitation to occur. Therefore, for any velocity it is the margin between the absolute pressure and the vapor pressure expressed as a fraction of the dynamic pressure that indicates whether or not cavitation will occur. This fraction can be written as $(P-P_v)/\rho\frac{V^2}{2}$ where the pressures are expressed in pounds per square foot.

In this report the data from the constant velocity experiments are plotted in the form of sound intensity as the ordinate against the pressure difference ($P-P_v$) as the abscissa. For convenience in comparing runs at different velocities, an additional scale of $(P-P_v)/\rho \frac{V^2}{2}$ is indicated along the abscissa. The magnitudes of the sound intensities will, of course, only hold for the particular velocity of the experiment.

IV. TUNNEL BACKGROUND NOISE

Measurements of the high frequency sound caused by the flow around the projectile must be made in the presence of noise generated by various parts of the tunnel flow circuit and its mechanical drive. Successful detection of the projectile noise requires that the noise inherent in the tunnel system be composed primarily of components of a different frequency range or that the magnitudes of any portions in the same frequency range are small relative to the projectile noise. Consequently, a "calibration" of the tunnel is necessary to determine the characteristics of the so-called "background" noise.

The calibration of the tunnel was made without the model or its supporting strut in place. Preliminary measurements were made over a wide pressure range at several velocities and for various frequency bands between 1 and 100 kilocycles. The microphone was mounted in the center of the lucite side window of the working section. (The same position as shown in Figure 2). It was oriented with the crystal diaphragms in planes parallel to the tunnel center line. These measurements showed a large amount of noise in the 1 to 5 kilocycle band and a slightly reduced amount in the 5 to 10 kilocycle band. Between 10 and 20 kilocycles, an appreciable further reduction was noted, while above 20 kilocycles, the noise was very much less than for any band below 20. Subsequent measurements with cavitating models in the working section showed that below 10 kilocycles, the magnitude of the noise from the cavitation was so small compared to the background noise, that accurate measurements were impossible. Between 10 and 20 kilocycles, measurements were possible, but the accuracy was less than that obtained above 20 kilocycles where the background noise could be neglected. Consequently, in order to avoid making background noise corrections, the measurements for this preliminary investigation were limited to frequencies between 20 and 100 kilocycles.

Figure 5 shows measurements of the background noise in the 20 to 100 kilocycle band obtained without the model or its supporting strut in the working section. In this test the sound intensity* was recorded with decreasing hydraulic pressure for a constant velocity of 50 feet per second. This is the maximum velocity used for any of the measurements with models in the working section. A pressure range of 26 to 6 pounds per square inch absolute was covered by the test. This curve shows the sound intensity to gradually increase with decreasing pressure until a maximum sound intensity is obtained at an absolute pressure of 11 pounds per square inch. As will be discussed, the increase in sound is probably due to hydraulic flow changes, either in some part of the main tunnel circuit away from the working section or in the auxiliary pressure control circuit. At pressures below 10 pounds per square inch, the sound intensity falls off rapidly until a minimum value is obtained, at about 7 pounds per square inch. At this minimum point the water in the Tunnel becomes clouded by an accumulation of air bubbles. Dissolution

* See footnote page 3

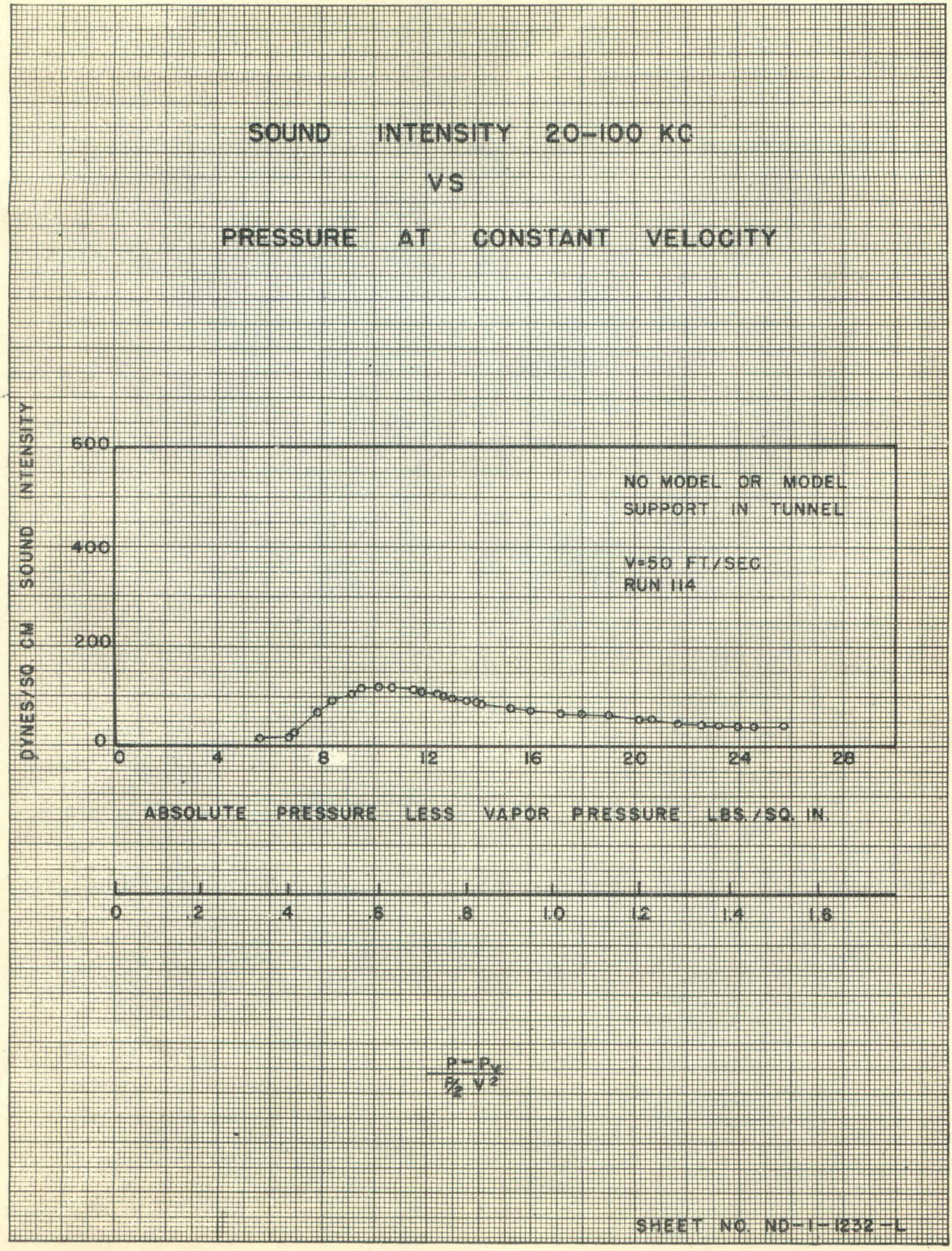
SOUND INTENSITY 20-100 KC
VS
PRESSURE AT CONSTANT VELOCITY
DYNES/SQ. CM SOUND INTENSITY
600
400
200
0
NO MODEL OR MODEL SUPPORT IN TUNNEL
V=50 FT/SEC
RUN 114
0
4
8
12
16
20
24
28
ABSOLUTE PRESSURE LESS VAPOR PRESSURE LBS./SQ. IN.
0
.2
.4
.6
.8
1.0
1.2
1.4
1.6
$\frac{P-P_v}{\frac{\rho}{2}V^2}$
SHEET NO. ND-1-1232-L

FIG. 5

of air from the water as it passes through the working section at low pressure, and the lack of complete re-dissolving of this air in the higher pressure zones of the tunnel circuit cause the accumulation. There is no leakage of air into the tunnel circuit. For this condition it was observed that the measured sound intensity was unaffected, either by a further decrease or by an increase in pressure so long as the air bubbles persisted. However, if the air was eliminated by operating at high pressures for a few minutes, the measurements shown in Figure 5 could be duplicated for pressures above 7 pounds per square inch. This behavior places a practical limit on the working section pressure for satisfactory sound measurements. For a velocity of 50 feet per second or more, this is not a severe limitation, since, for most projectiles, cavitation develops at pressures above the limit. At low velocities, however, it is a handicap. Provisions are being made for de-aerating the water used in the Water Tunnel circuit to facilitate future measurements.

The factors contributing to background noise measured for pressures above 7 pounds per square inch, are essentially of two types. Mechanical noises from the rotating machinery associated with the installation make up the first type, and hydraulic noises in main tunnel circuit, in the auxiliary pressure control circuit, and in the circulating pumps for both circuits make up the second type. It is reasonable to assume that the mechanical noises are constant for a fixed tunnel speed. The hydraulic noises, however, can be expected to vary as the pressure is reduced because of flow discontinuities, such as cavitation, at the pump impeller blades, in the vaned elbows and honeycombs, or at the control valves in the pressure control circuit. The increase in sound intensity with decreasing pressure shown in Figure 5 is probably produced by these latter causes.

During the course of the investigations it was found that the background noise was sometimes greater or less than the values shown in Figure 5 (for the same velocity, of course), depending upon how the valves in the auxiliary pressure control circuit were adjusted. Where possible variations were avoided by duplicating the settings from run to run, but this was not always feasible, so brief checks of the background sounds were frequently made. It was found that the maximum level measured for any valve position was small compared to total sound measured with cavitating models in the working section. This is important because since the sound intensity measured is approximately proportional to the root-mean-square value of the acoustic pressure, a background noise one half as great as the noise due to cavitation will only add about 10% to the magnitude of the total sound measured during cavitation. Consequently, it is possible to neglect the influence of the background noise.

FIGURE 6

2" DIAMETER MODEL PROJECTILE
WITH HEMISPHERICAL NOSE

FIGURE 7

2" DIAMETER MODEL PROJECTILE
WITH "HALFBODY" STREAMLINED NOSE

V. THE VARIATION OF SOUND INTENSITY WITH THE BEGINNING AND GROWTH OF CAVITATION

Measurements of the high frequency noise were made with three models in the working section of the Water Tunnel. These models were made up with the same body and tail but with three different noses, a hemispherical nose, a streamline (half body) nose, and a truncated hemispherical nose. Photographs of the model with the hemispherical and the streamline nose are shown in Figures 6 and 7 and the profiles of all three noses are shown in Figure 8.* Complete details of these models will be found in another Water Tunnel report.[2] As stated in Section II, the hydrophone is mounted on the working section window and records the sound at that point. The hydrophone orientation was the same as used to obtain the background noise calibration, with the crystal diaphragms in planes parallel to the tunnel center line. Figure 9 shows the position of the hydrophone and of the models as installed for testing. The diagram for the hemispherical nose corresponds identically to the setup pictured in Figure 2.

Measurements of the sound intensity# in the 20 to 100 kilocycle frequency band for a variable pressure in the working section are shown in Figure 10 for the model with the hemispherical nose. The coordinates for the diagrams are sound intensity in dynes per square centimeter and the pressure difference $(P-P_v)$. A scale for $(P-P_v)/\rho\frac{V^2}{2}$ is also shown. These data were obtained with a velocity of 50 feet per second and with the model aligned with the flow, and also yawed at 2.5° and 5°. Two runs obtained at different times are shown for both the zero degree yaw and the 2.5° yaw conditions. The sound intensities are not corrected for background noise. Referring to the top diagram for zero yaw, it is seen that the sound intensity increases gradually with decreasing pressure until at about 13 to 14 pounds per square inch when a sharp rise in sound is measured. The increased sound level is several times the level at higher pressures and corresponds to the beginning of cavitation on the nose of the projectile. Simultaneous observations of the cavitation and the sound level showed that the noise reached a peak when a very stable but narrow band of cavitation was visible around the nose. Figure 13 shows the model under these conditions of velocity and pressure for the same zero yaw angle. Note that the photograph was obtained with $(P-P_v)\ \rho\frac{V^2}{2} = 0.63$ and the peak noise in Figure 10 occurs when this fraction is about 0.65.

* The streamline shape is derived for ideal flow conditions by assuming a single "source" in rectilinear flow. Since this consideration leads to a body with a uniform diameter only at infinity, a faired transition curve was used between a point 1.2 inches back from the nose tip and a point 2.5 inches back to the 2" diameter body section of the projectile. Dr. H. J. Stewart of the California Institute of Technology is responsible for calculating this profile.

See footnote page 3

With further reduction in pressure, the measured sound intensity decreases from the peak value down to about the same value as before cavitation began. Note that this reduced sound is obtained even though the zone of cavitation has grown in size. Figure 14 shows the model as it appeared with $(P-P_v)$ equal to about 9.5 pounds per square inch, the pressure for the very much reduced sound intensity. This reduction may be the result of an actual change in the character of the noise produced as the cavitating zone grows, or it may be caused by a higher attenuation for the water-vapor zone than for the water alone, thus tending to prevent a portion of the noise from reaching the hydrophone as cavitation grows. The effect of the accumulation of air bubbles cited in Section IV tends to substantiate the latter idea, but further investigations will be necessary to determine the true cause of this behavior.

At still lower pressures a second peak is obtained. This one occurs when the strut supporting the model begins to cavitate. Figure 15 shows the model at the pressure for the second peak. Note that cavitation bubbles appear on the surface of the shield. Note, also, the advanced stage of the cavitation at the nose.

Again the sound intensity falls off as the pressure is dropped until its magnitude is almost negligible. This reduction is accompanied by an accumlation of air, as was described in the previous section and as is shown by the bubbles distributed throughout the flow in the photograph of Figure 16.

Similar results are obtained when the model is yawed except that the nose cavitates at a higher pressure and cavitation on the tail fin surfaces becomes more important. For zero yaw cavitation was observed on the fins, but the noise from this source could not be distinguished in the presence of the nose and shield cavitation. The center diagram on Figure 10 for a 2.5° yaw angle shows a peak in the sound intensity that occurs when the lee side of the nose and the lee side of the vertical tail fins cavitate simultaneously. Figure 17 illustrates the type of cavitation that is obtained on the fins. This photograph was taken with a 10° yaw angle so the cavitation is more severe than was obtained at 2.5° yaw. The lower diagram for 5° yaw shows a more gradual increase in sound intensity, as the pressure is reduced, with several irregularites in the curve. The pressures at which the tail fins and the nose cavitate are indicated. The other irregularities are not positively identified but it is thought that cavitation at the junction gap between the model and its supporting strut may be one of the contributing factors. This gap is obtained for large yaw angles because the strut remains fixed while the model orientation is changed. Since the strut position does remain unchanged, its behavior is not affected by yawing the model. Consequently, in each of the three diagrams of Figure 10 the peak noise caused by the strut occurred at identical pressures.

The 2 sets of measurements plotted for zero yaw, and also for 2.5° yaw, show discrepancies in both the cavitating and the non-cavitating pressure ranges. Under cavitating conditions there are deviations in the peak sound intensities of as much as 25% of maximum measured value. Measurements near the peak intensities are subject to some errors because the actual formation of the cavitation bubbles gives a fluctuating rather than a steady state condition. Rather large fluctuations of the noise occur which limit the accuracy and may be responsible for the differences shown here. Under non-cavitating conditions the percentage deviations between the curves are larger. They represent a difference in background noise which, as discussed in Section IV, is probably caused by the positioning of the pressure control circuit valves. In no case, however, was the background noise as much as 50% of the peak noise measured with the onset of cavitation so this behavior will not account for any general difference between the two curves.

Figure 11 shows curves of sound intensity plotted against pressure difference ($P-P_v$) for the model with the streamline (half body) nose at zero yaw angle and at 5° yaw angle. These measurements were also made with a tunnel velocity of 50 feet per second and include the 20 to 100 kilocycle frequency band. At zero yaw the sound intensity does not become large until the pressure is reduced to 7.5 pounds per square inch absolute. At this pressure the shield begins to cavitate. This nose does not cavitate until the pressure is so low that air bubbles begin to accumulate. As discussed in Section IV, the presence of air bubbles in the Tunnel lowers the sound intensity at the hydrophone, so measurements at this very low pressure have no significance. Consequently, no noise values were recorded. Cavitation on the afterbody and tail fins occurs in the same range of pressures covered by the peak due to the strut noise and, therfore, cannot be distinguished.

The lower diagram in Figure 11 for a 5° yaw angle shows the sound intensity to rise appreciably at about 18 pounds per square inch. This seems to correspond to the cavitation on the lee side of the tail fins which was observed at about the same pressure. With a further reduction in pressure, a second peak in intensity was observed which was not identified during the test. Finally a high peak is obtained when the shield and the lee side of the nose cavitate simultaneously.

As an illustration of the usefulness of these measurements note that the two diagrams in Figure 11 compared with Figure 10 show two important points. The first is the beneficial effect of streamlining the nose. The second is that this benefit is cancelled as the yaw angle increases because the tail fin cavitation still causes noise at high pressures. Since yaw angles of 2.5° and possibly 5° can be obtained with an actual projectile, the afterbody and the tail fins assume relatively more importance as the nose performance is improved.

The fact that cavitation becomes visible at the same pressure at which the sound intensity increases is one of the important findings of the investigation, since it means that visual measurements of the onset of cavitation are almost as good as actual sound measurements in determining limiting pressures and velocities for sound free operation. As a result, it is interesting to point out that visual measurements of other noses with ellipsoidal and ogive profiles showed cavitation characteristics similar to those of the streamline nose and hence can be expected to produce similar noise curves. This in itself is important because a nose with a simple profile curve should be easier to manufacture than the streamline type.

Sound measurements taken with the truncated hemisphere nose on the model are shown for zero yaw in Figure 12. These data were obtained at 41 feet per second and include the 20 to 100 kilocycle frequency band. This nose was purposely selected because it cavitated well above atmospheric pressure making it possible to determine whether or not the pressure range influenced the shape of the sound curves. Note that the pressure range covered by this entire test is above atmospheric pressure while in Figures 10 and 11 cavitation was obtained only at pressures below atmospheric pressure. Since the truncated hemispherical nose cavitates at such a high pressure, no other part of the model or its support cavitated within the range of the test. Also, because the pressure is above atmospheric, there is no dissolution of air from the main flow about the model. In general the curve for the truncated hemisphere has the same characteristics as the curve for the hemispherical nose. As the pressure is reduced until cavitation begins, the sound intensity increases abruptly while with continued growth of the cavitating zone, the intensity finally drops off.

When examined in detail it is seen that the results with this nose differ from the results with the other noses. The increase in sound intensity at the beginning of cavitation is much more sudden in Figure 12 than in Figures 10 or 11. Furthermore the peak sound intensity occurs sometime after cavitation begins and is preceded by a slight reduction in intensity. These differences are attributed to a difference in the way cavitation first occurs and grows. Observations during the tests showed that the initial stages of the development of the cavitation zone looked very different for this sharp edged nose than for the smooth noses. For a hemishperical nose the first visable cavitation appears to lie on the surface of the nose whereas for a square cut nose, the first visable cavitation occurs in the fluid slightly away from and aft of the nose tip.

Observe that the noise intensity at the highest pressure of the test is very low, indicating the order of magnitude of the background noise in this pressure range.

In Figure 12 two curves are shown, one for decreasing pressure in

the working section and the other for increasing pressure. The agreement between the two curves is good except at the boundary between cavitating and non-cavitating conditions. As the pressure is lowered the sound increases suddenly to a high value as cavitation occurs. On the other hand, if the pressure is increased, the cavitation seems to persist beyond this first discontinuity, thus causing a hysteresis loop. This loop could be retraced readily. Similar hysteresis loops are shown for two other runs in Figure 19. Run 116-C is for the hemispherical nose at a 5° yaw (See Figure 10) and run 120 is another determination for the truncated hemisphere nose at $\psi = 0^{\circ}$ yaw. For each of these three examples observations of the pressure at which cavitation was first visible and the pressure at which it disappeared, confirmed the existence of the hysteresis effect.

As indicated in Section III, the measurements shown in Figures 10, 11, and 12 can be used to calculate the performance of the projectile at different velocities, and thus to determine the limiting velocities for sound free operation. Such a calculation was made for tests using the model with the hemispherical nose and the streamline nose. Figure 18 shows data for zero yaw taken from Run 116-A (in Figure 10) and Run 113 (in Figure 11), replotted as sound intensity vs. velocity for a constant pressure. A pressure of 21 pounds per square inch absolute was used, a value which would be realized if the submergence in sea water was 15 feet. The sound intensity values were not corrected for the influence of velocity so no scale is shown and the resulting curves should be interpreted qualitatively.

Referring to the curve for the hemispherical nose, it is seen that for velocites below 61 feet per second, the noise is nearly uniform and relatively low. At about 61 feet per second the intensity begins to grow, rising sharply to a peak at about 69 feet per second (41 knots). Here the cavitation forms a narrow, stable band around the nose. With additional velocity the noise drops and then begins to rise again as the supporting strut begins to cavitate. Of course, only the first peak is significant in discussing the behavior of the actual projectile. With the streamline nose, on the other hand, no increase in noise occurs until the velocity reaches 76 feet per second and, in fact, the rise beginning here is caused by cavitation of the supporting strut. The nose itself does not cavitate until even higher velocities are reached. This diagram emphasizes the benefits possible by streamlining the nose.

As already pointed out, at yaw angles of 2.5° or 5°, cavitation on the tail fins and rudders occurs at high pressures if the speed is fixed. If data for 2.5° and 5° yaw were also plotted on the constant submergence variable velocity basis, the noise peaks caused by the fins cavitating would occur at much lower velocities than the peaks due to the nose. Thus the maximum velocity, as well as the minimum pressure at which noise free operation is possible, depends upon the tail surface behavior.

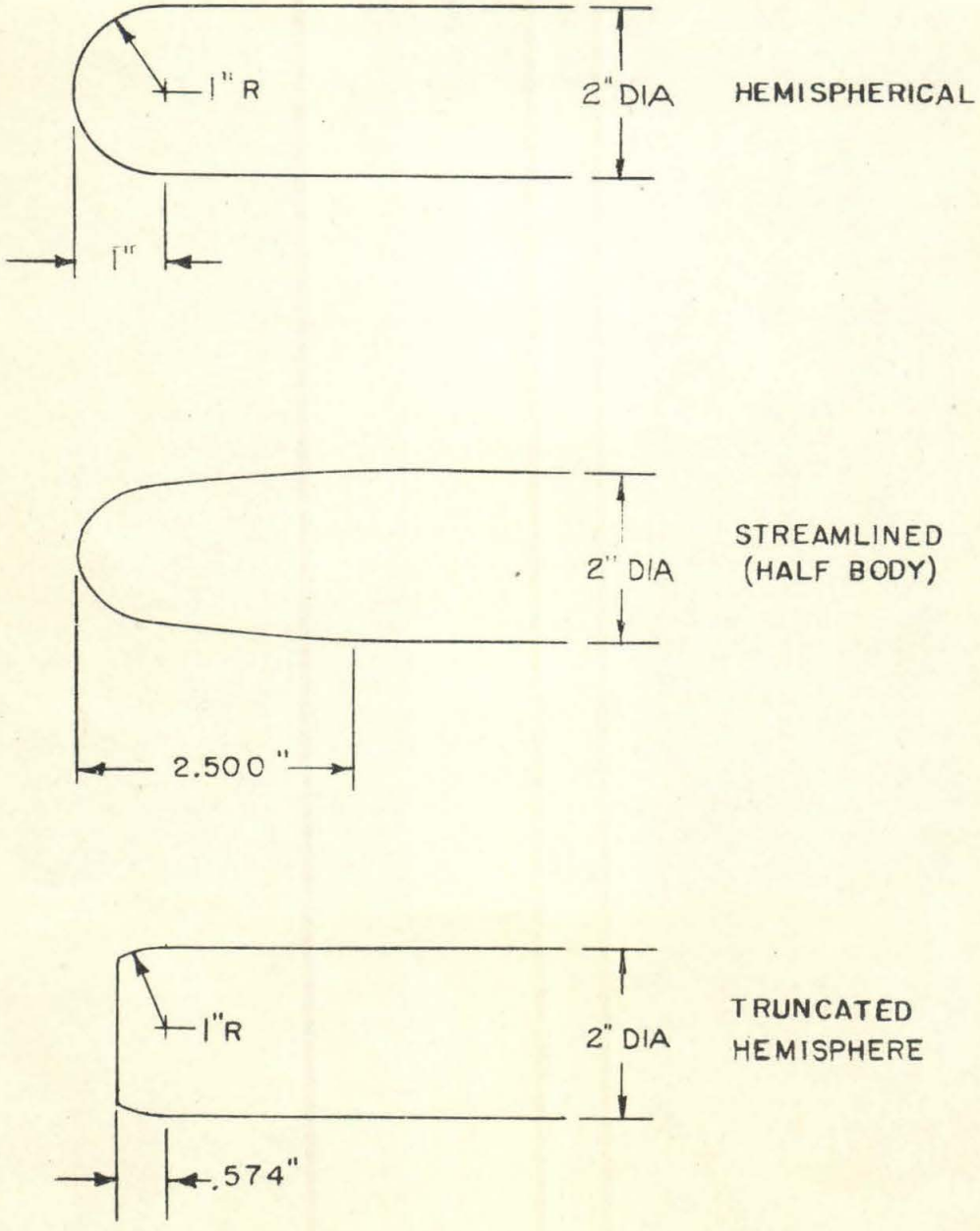

HYDRAULIC MACHINERY LABORATORY CALIFORNIA INSTITUTE OF TECHNOLOGY		
DR H C Y 8-28-43	PROFILES OF PROJECTILE NOSE SHAPES	SCALE HALF
CH		ND 8-1222 -L
AP		

FIG. 8

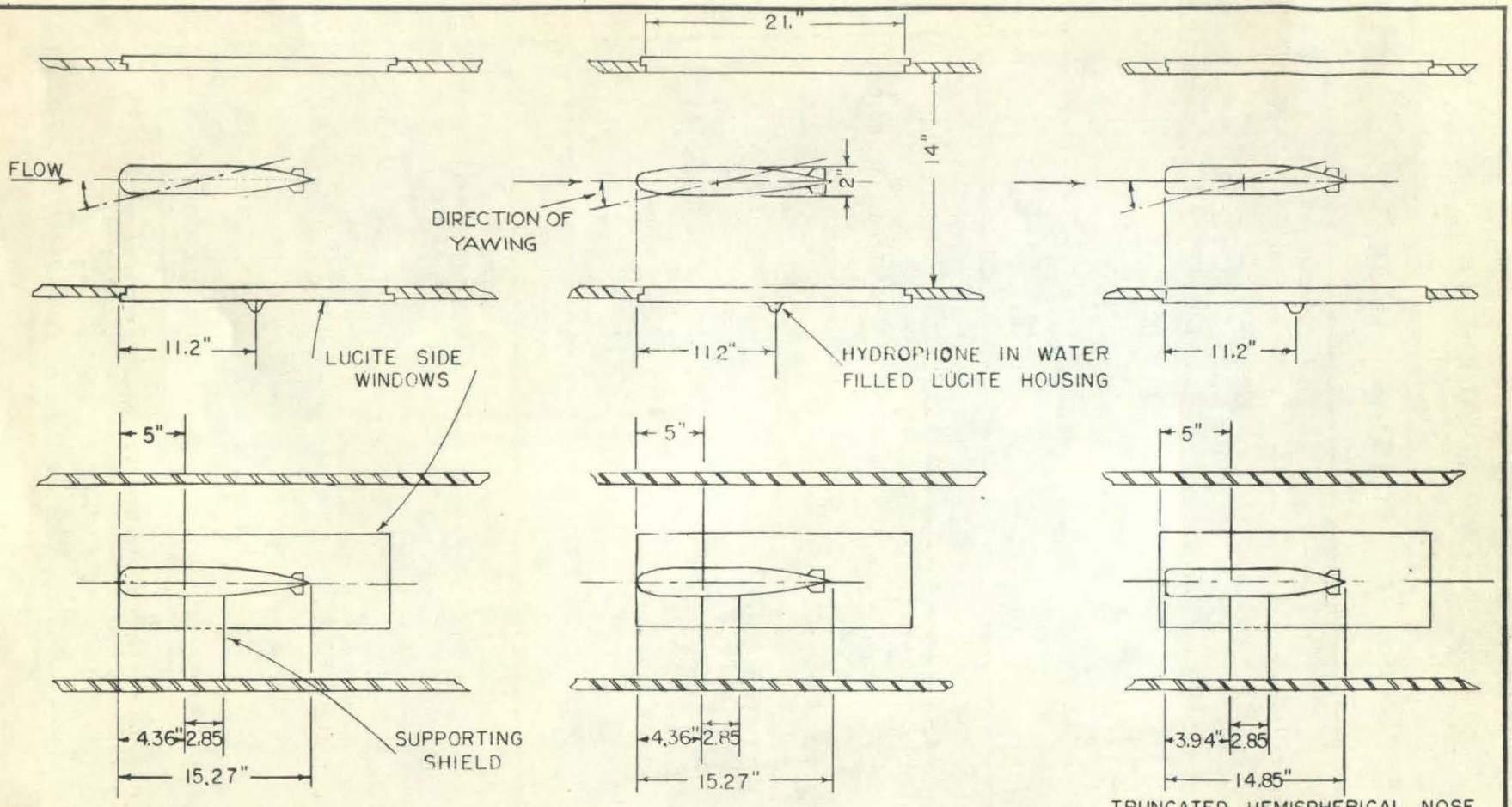

HEMISPHIERICAL NOSE
(ND-8.7-2)
RUNS 117-A
116-A
116-B
116-B'
116-C

STREAMLINED (HALFBODY) NOSE
(ND-8.19-1)
RUNS 113
115

TRUNCATED HEMISPHERICAL NOSE
(8.22-1)
RUN 118

HYDRAULIC MACHINERY LABORATORY
CALIFORNIA INSTITUTE OF TECHNOLOGY
PASADENA, CALIFORNIA

DIMENSIONS FOR TEST INSTALLATIONS

DR C.M.E. 8-31	SCALE 1/2 = 1"
CH	ND 1223-U
AP	

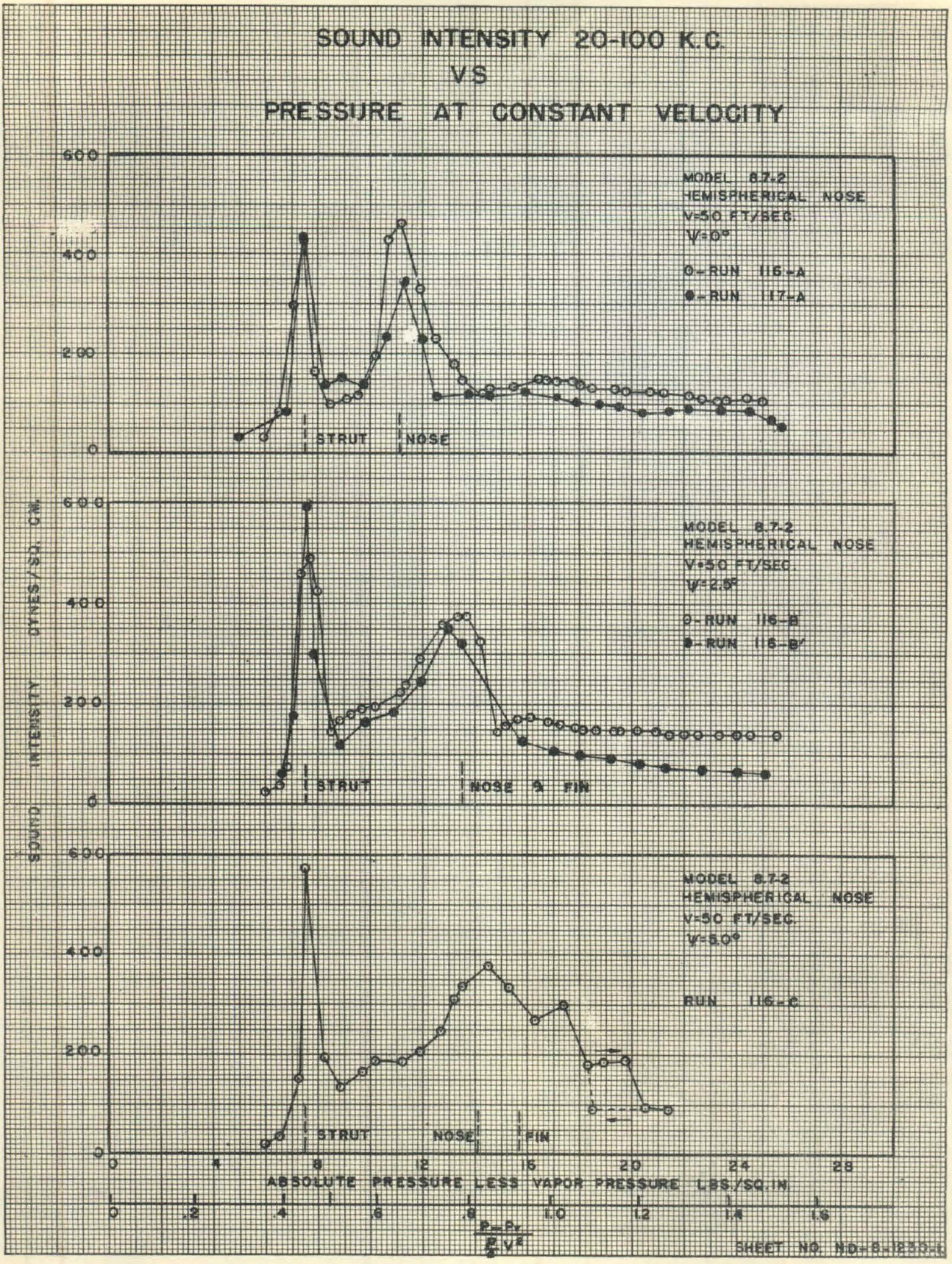
SOUND INTENSITY 20-100 K.C.
VS
PRESSURE AT CONSTANT VELOCITY
MODEL 8.7-2
HEMISPHERICAL NOSE
V=50 FT/SEC.
V=0°
O-RUN 116-A
●-RUN 117-A
STRUT
NOSE
MODEL 8.7-2
HEMISPHERICAL NOSE
V=50 FT/SEC.
V=2.5°
O-RUN 116-B
●-RUN 116-B'
STRUT
NOSE & FIN
MODEL 8.7-2
HEMISPHERICAL NOSE
V=50 FT/SEC.
V=5.0°
RUN 116-C
STRUT
NOSE
FIN
SOUND INTENSITY DYNES/SQ. CM.
ABSOLUTE PRESSURE LESS VAPOR PRESSURE LBS./SQ.IN.
SHEET NO. ND-8-1230-1

FIG 10

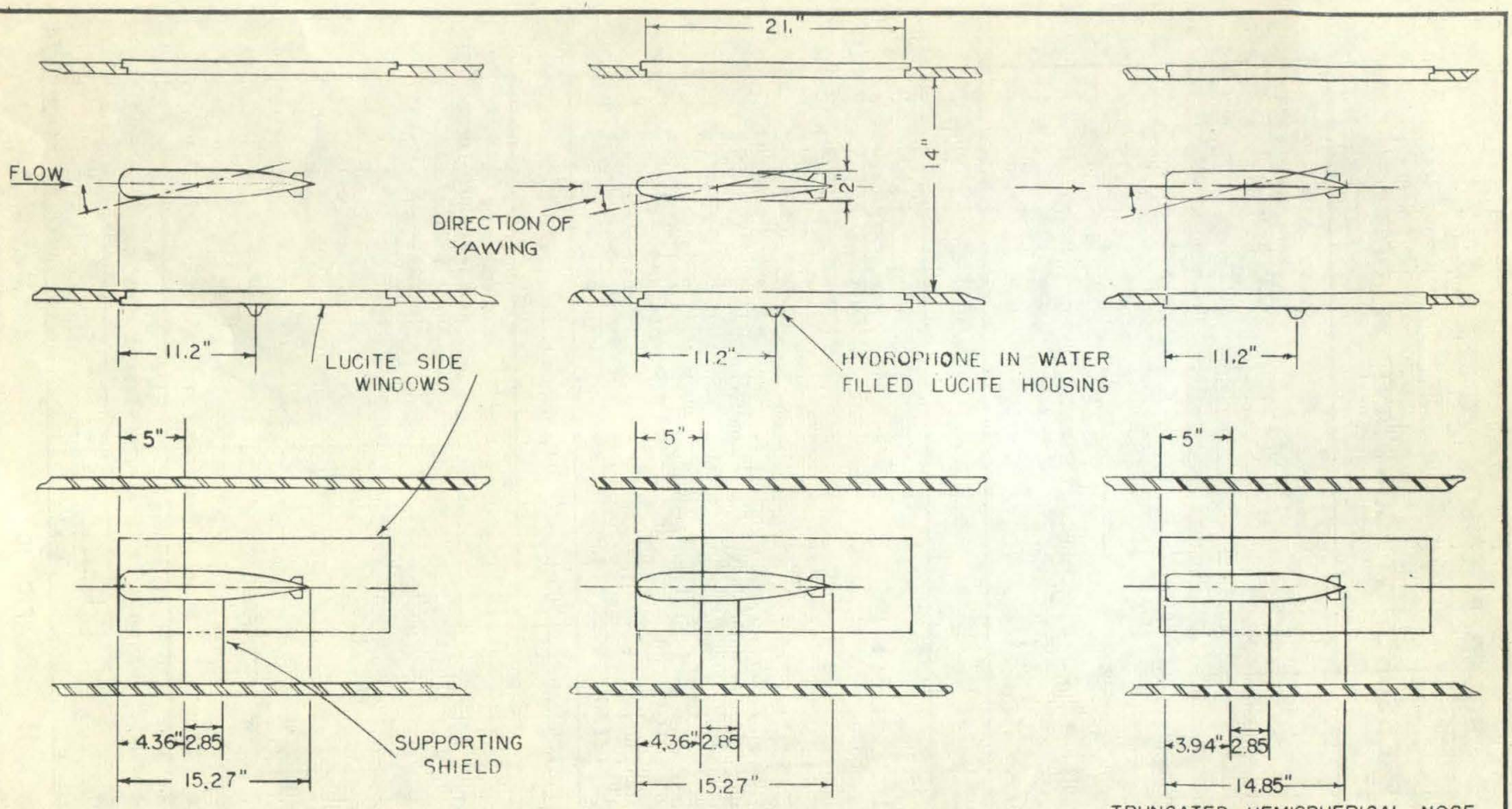

HEMISPHIERICAL NOSE
(ND-8.7-2)
RUNS 117-A
116-A
116-B
116-R'
116-C

STREAMLINED (HALFBODY) NOSE
(ND-8.19-1)
RUNS 113
115

TRUNCATED HEMISPHERICAL NOSE
(8.22-1)
RUN 118

HYDRAULIC MACHINERY LABORATORY CALIFORNIA INSTITUTE OF TECHNOLOGY PASADENA, CALIFORNIA	
DIMENSIONS FOR TEST INSTALLATIONS	
DR C.M.E. 8-31	SCALE 1/2"=1"
CH	ND 1223-U
AP	

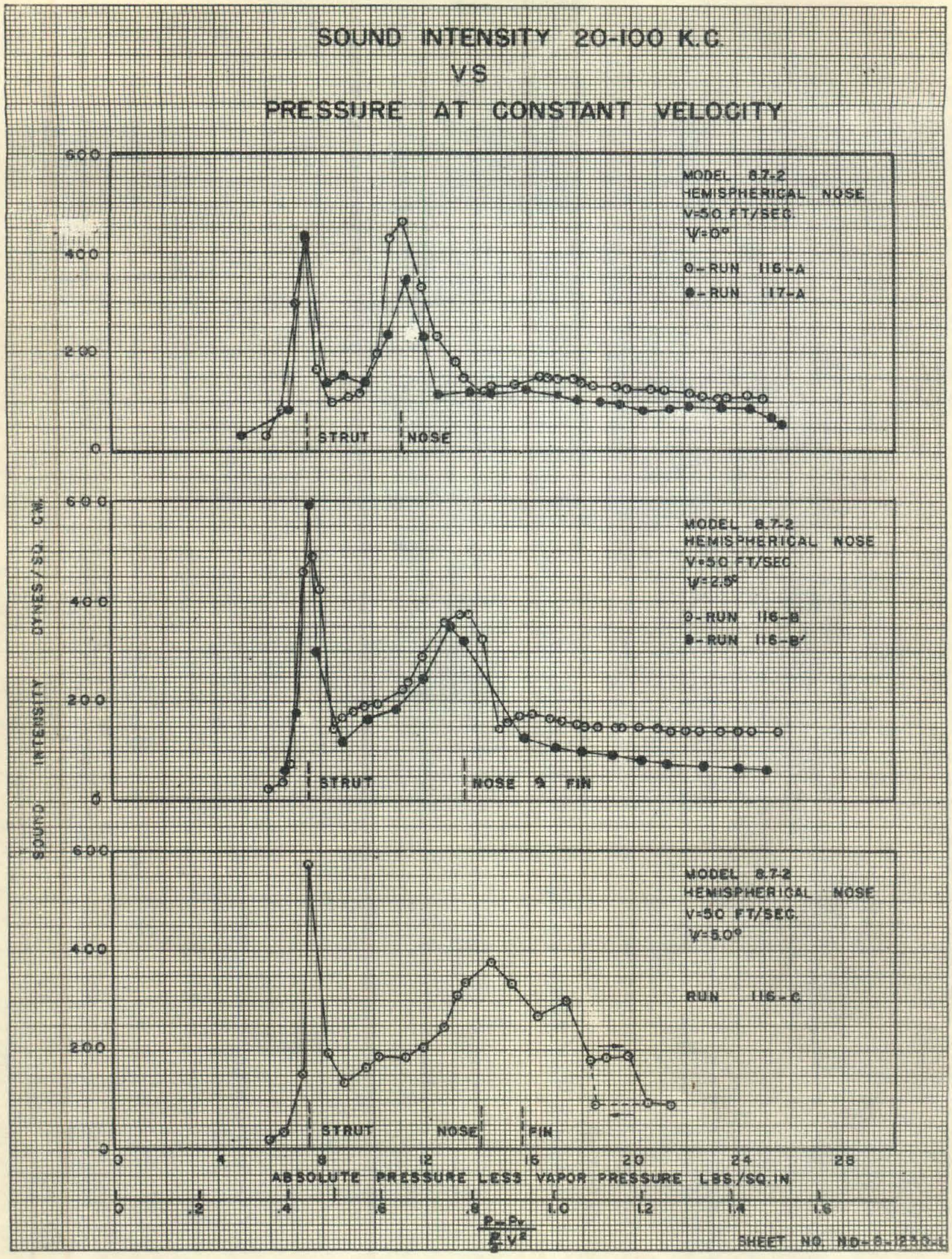
SOUND INTENSITY 20-100 K.C.
V.S
PRESSURE AT CONSTANT VELOCITY
MODEL 8.7-2
HEMISPHERICAL NOSE
V=50 FT/SEC.
ψ=0°
O-RUN 116-A
●-RUN 117-A
STRUT
NOSE
MODEL 8.7-2
HEMISPHERICAL NOSE
V=50 FT/SEC.
ψ=2.5°
O-RUN 116-B
●-RUN 116-B'
STRUT
NOSE & FIN
MODEL 8.7-2
HEMISPHERICAL NOSE
V=50 FT/SEC.
ψ=5.0°
RUN 116-C
STRUT
NOSE
FIN
SOUND INTENSITY CYCLES/SQ. CM.
ABSOLUTE PRESSURE LESS VAPOR PRESSURE LBS./SQ.IN.
SHEET NO. NO-8-1230-C

FIG 10

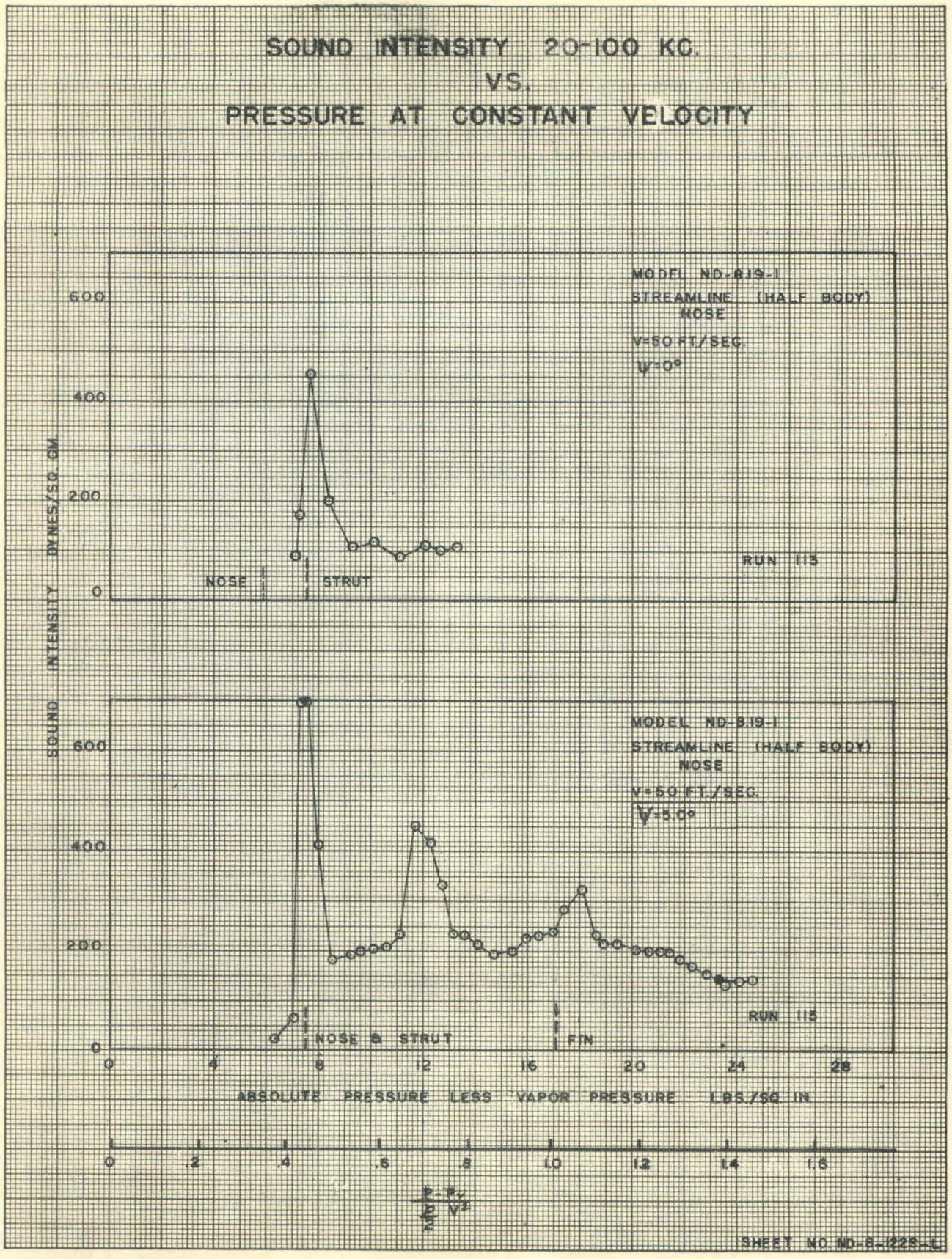
SOUND INTENSITY 20-100 KC.
VS.
PRESSURE AT CONSTANT VELOCITY
MODEL ND-8.19-1
STREAMLINE (HALF BODY)
NOSE
V=50 FT./SEC.
ψ=0°
RUN 115
NOSE
STRUT
SOUND INTENSITY DYNES/SQ. CM.
600
400
200
0
MODEL ND-8.19-1
STREAMLINE (HALF BODY)
NOSE
V=50 FT./SEC.
ψ=5.0°
RUN 115
NOSE & STRUT
FIN
0
4
8
12
16
20
24
28
ABSOLUTE PRESSURE LESS VAPOR PRESSURE LBS./SQ. IN.
0
.2
.4
.6
.8
1.0
1.2
1.4
1.6
P-Pv / ½ρV²
SHEET NO. ND-8-1228-5

FIG 11

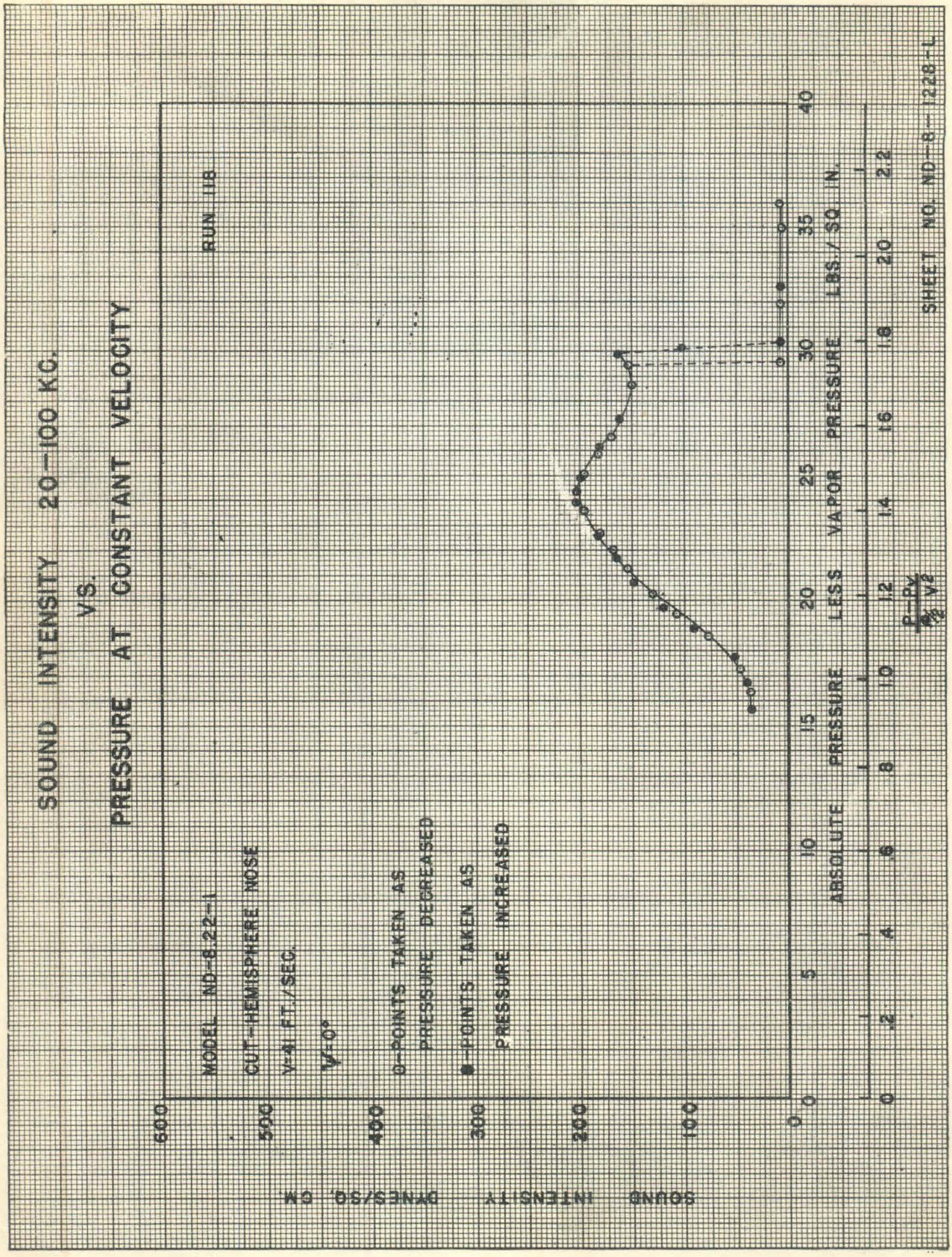
SOUND INTENSITY 20—100 KC.
VS.
PRESSURE AT CONSTANT VELOCITY
RUN 18
MODEL NO-8.22-1
CUT-HEMISPHERE NOSE
V=41 FT./SEC.
M=0
0-POINTS TAKEN AS PRESSURE DECREASED
●-POINTS TAKEN AS PRESSURE INCREASED
SOUND INTENSITY DYNES/SQ. CM.
ABSOLUTE PRESSURE LESS VAPOR PRESSURE LBS./SQ. IN.
SHEET NO. ND-8-1228-L

FIG. 12

FIGURE 13

$$\frac{P-P_v}{\rho \frac{V^2}{2}} = 0.63$$

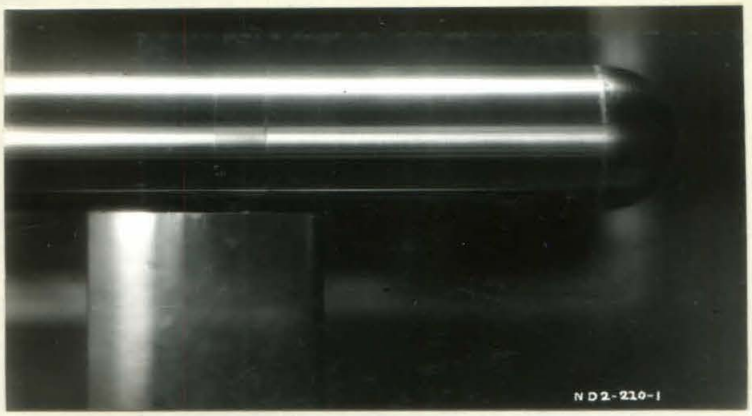

FIGURE 14

$$\frac{P-P_v}{\rho \frac{V^2}{2}} = 0.57$$

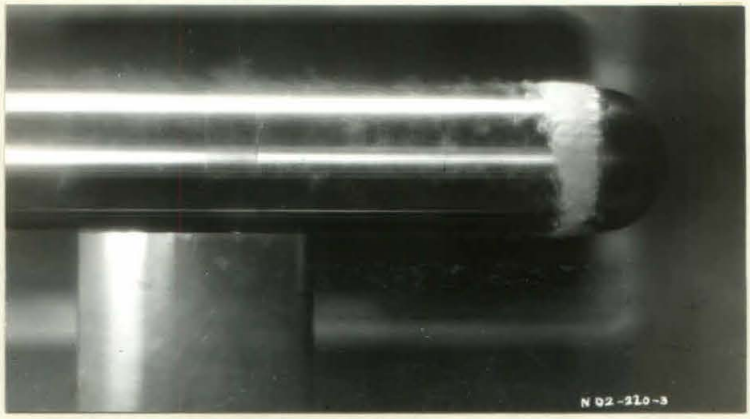

FIGURE 15

$$\frac{P-P_v}{\rho \frac{V^2}{2}} = 0.43$$

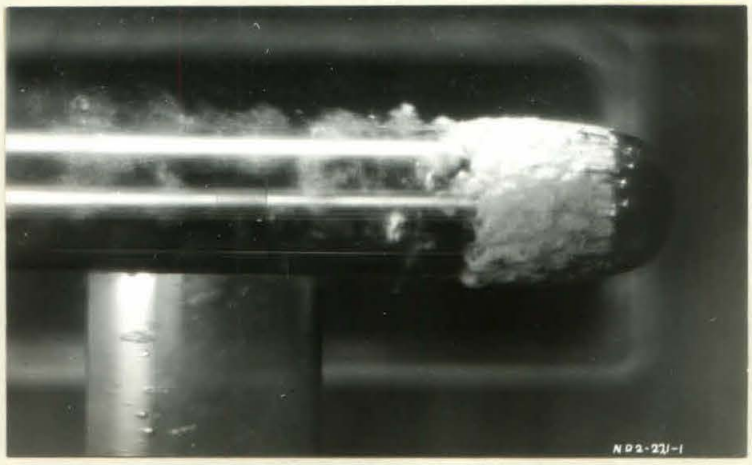

FIGURE 16

$$\frac{P-P_v}{\rho \frac{V^2}{2}} = \text{LESS THAN } 0.35$$

FIGURES 13 THROUGH 16 SHOW THE DEVELOPMENT OF THE CAVITATION ON A HEMISPHERICAL NOSE AS THE PRESSURE IS REDUCED WITH A CONSTANT VELOCITY OF 50 FEET PER SECOND.

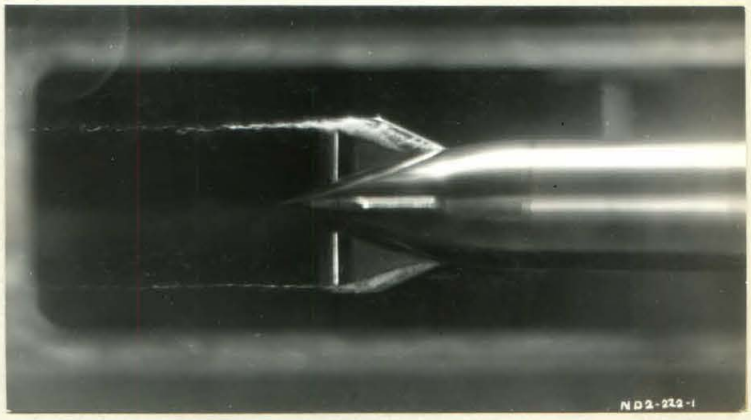

FIGURE 17

CAVITATION ON THE LEE SIDE OF THE TAIL FINS OF A MODEL YAWED AT 10° IN A 50 FOOT PER SECOND STREAM.

SOUND INTENSITY (20-100 KC.) VS. VELOCITY AT CONSTANT SUBMERGENCE OF 15 FEET

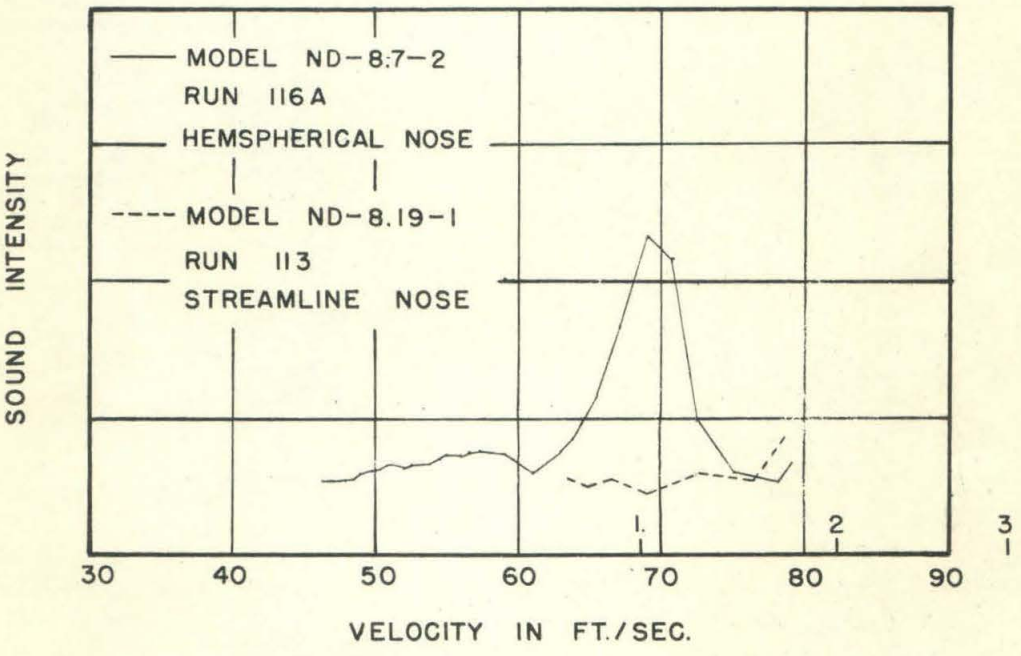

NOTE: THESE CURVES ARE CALCULATED FROM CONSTANT VELOCITY RUNS. MAGNITUDE OF SOUND INTENSITY IS NOT CORRECTED FOR VELOCITY.

1.- HEMISPHERICAL NOSE CAVITATES

2-STRUT CAVITATES

3-STREAMLINE NOSE CAVITATES

SHEET NO ND-8-1349-L

FIG 18

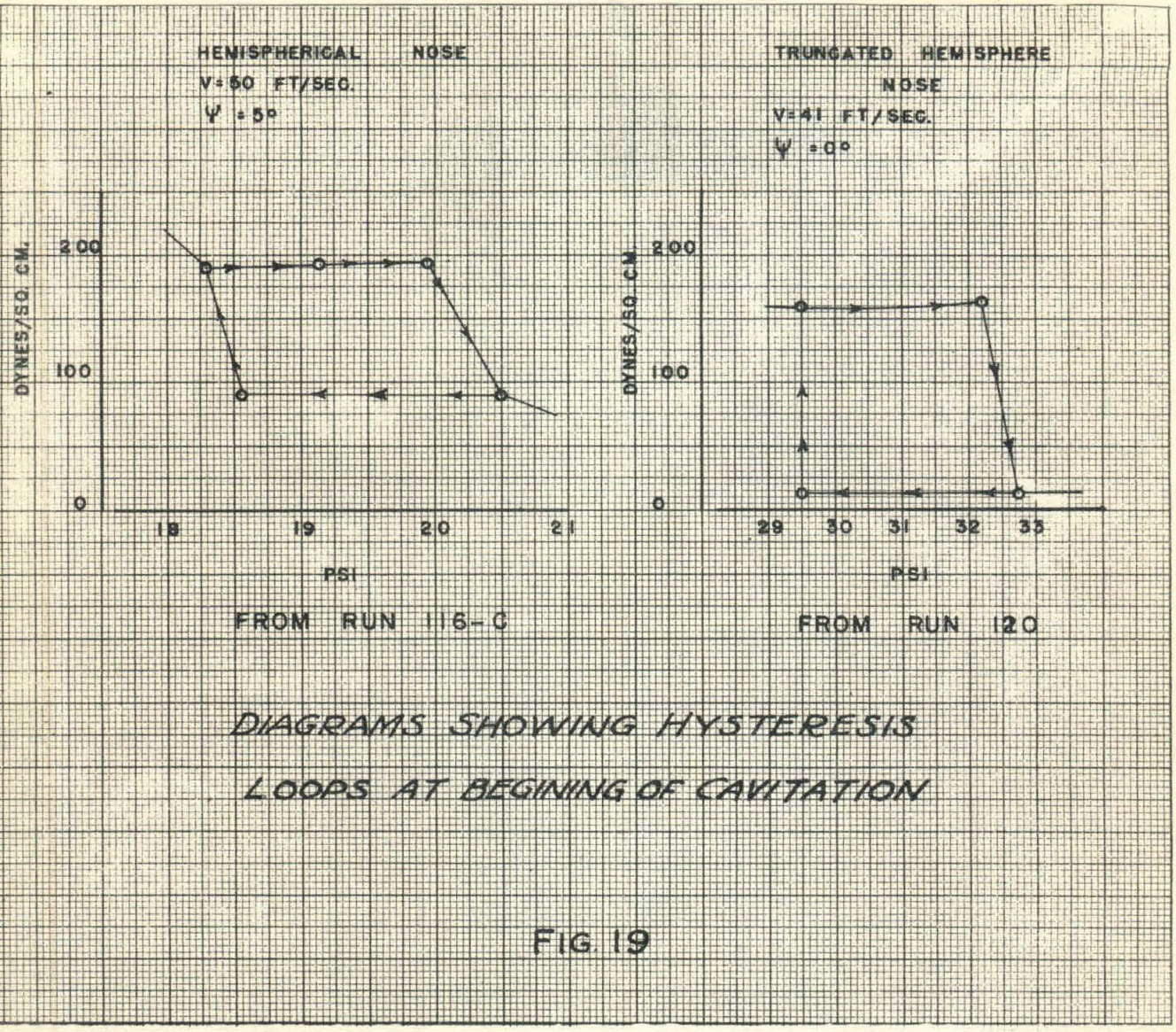

DIAGRAMS SHOWING HYSTERESIS LOOPS AT BEGINING OF CAVITATION

FIG. 19

VI. FREQUENCY DISTRIBUTION MEASUREMENTS — EFFECT OF RELATIVE POSITION OF HYDROPHONE AND MODEL

One of the objectives of this preliminary investigation was to measure the distribution of the high frequency noise when cavitation occurs. Obtaining significant measurements of this type is very difficult since the hydrophone is separated from the sound source by water and the lucite tunnel window and since it is possible for the geometry of the installation to cause reflection patterns that will bias the determinations. As a result the relative position of the hydrophone and the sound source has an important influence, and a single set of measurements for one installation cannot be relied upon to indicate accurately either the magnitude or the distribution of the actual noise generated in the working section. This handicap was not present for the measurements reported in Section V because the main interest lay in the relative amount of noise obtained over a wide frequency band with and without cavitation. Neither the absolute magnitudes of the measured intensities nor the distribution within the band covered was of particular significance there.

Because of the above considerations, a series of experiments was performed with different hydrophone and projectile positions. The projectile with the truncated hemispherical nose was used for all the tests in combinations illustrated to scale in Figure 20. Two types of changes were made. First, in Run 127 the projectile position was left unchanged and the hydrophone was moved closer to the model nose. Second, in Run129 the hydrophone was left at the center of the lucite window and the projectile was moved back on its supporting strut. In each case the same hydrophone orientation was used as heretofore, with the planes of the crystal diaphragms parallel to the Tunnel center line. For the first method the conditions inside the tunnel were not disturbed so that the measured noise should give a definite indication of the effect of hydrophone position. For the second the nose cleared the supporting strut sufficiently to avoid interference with the development of cavitation (as was verified visually), and furthermore the nose cavitated at a pressure so high that no other part of the model or the strut cavitated. Consequently, it is believed that this test should also give a reliable indication of the effect of hydrophone position.

Figures 21, 22, and 23 show several runs made with the projectile and hydrophone arrangements shown in Figure 20. Figure 21, for Run 123, gives the total intensity* in the 20–100 kilocycle band measured with the same installation as for Run 124–C. The measurements for Run 123 are within the cavitating pressure range with a velocity of 50 feet per second. The curves show that the contributions of the various frequency bands are not uniform

* See footnote page 3

and that the predominant intensities are measured in the 30 to 40 kilocycle band. Figure 22 is a set of curves showing comparisons of the noise measured in each frequency band for the three different arrangements shown in Figure 20. Figure 23 shows the total noise measured in the 20-100 kilocycle band for the same three installations. The runs in Figures 22 and 23 were made at 41 feet per second. Figure 23 shows that the magnitude and location of the peak of measured sound intensity for the entire band changes when the hydrophone position is shifted. Figure 22 shows that for any narrow band of frequencies, the location of the peak intensity and the shape of the curves are almost unchanged, although there are changes in the magnitudes of the sound. This indicates that the frequency response of the measuring system is a function of the position of the hydrophone. This condition is expected if a complex standing wave pattern exists. The standing wave pattern is probably a simpler function of frequency directly opposite the nose than it is some distance down the tunnel. If this is true, it may be expected that Run 129 gives a closer approximation of the true state of affairs than either Run 127 or 124-C.

Run 129 shows the sound intensity near the inception point (28 pounds per square inch absolute) to decrease with decreasing frequency. This becomes less pronounced as the pressure is decreased until at 16 pounds per square inch absolute, the intensity is almost uniform over the entire frequency range considered.

As was previously stated, Figure 22 shows that the pressure corresponding to the peak intensity for a narrow frequency band is not changed by moving the hydrophone or the model. This indicates that for this shape of nose, there is a certain pressure that will correspond to peak intensity of a given frequency. The association of the peak intensity with a definite pressure for a given frequency probably holds for other shapes than the one used for these experiments, but the exact relationship will be expected to vary.

In Figure 23 two curves for sound intensity in the range of 20-100 kilocycles for Run 129 are shown. One was obtained by plotting the observed points, the other by plotting of square root of the sum of the squares of the intensities observed in the individual frequency bands. Very good agreement is obtained in the region between 14 and 22 pounds per square inch absolute. Between 22 and 28 pounds per square inch absolute differences of about 10% appear between the two curves. An explanation of this difference may be obtained by examination of Figure A-17 in the appendix. It is seen here that the response of the filter in the range 20-100 kilocycles is slightly better at high frequencies than at low frequencies. Hence, at higher pressures where the high frequencies predominate, the attenuation is less than the average value (see Appendix Page 4a), making the calculated intensities slightly high.

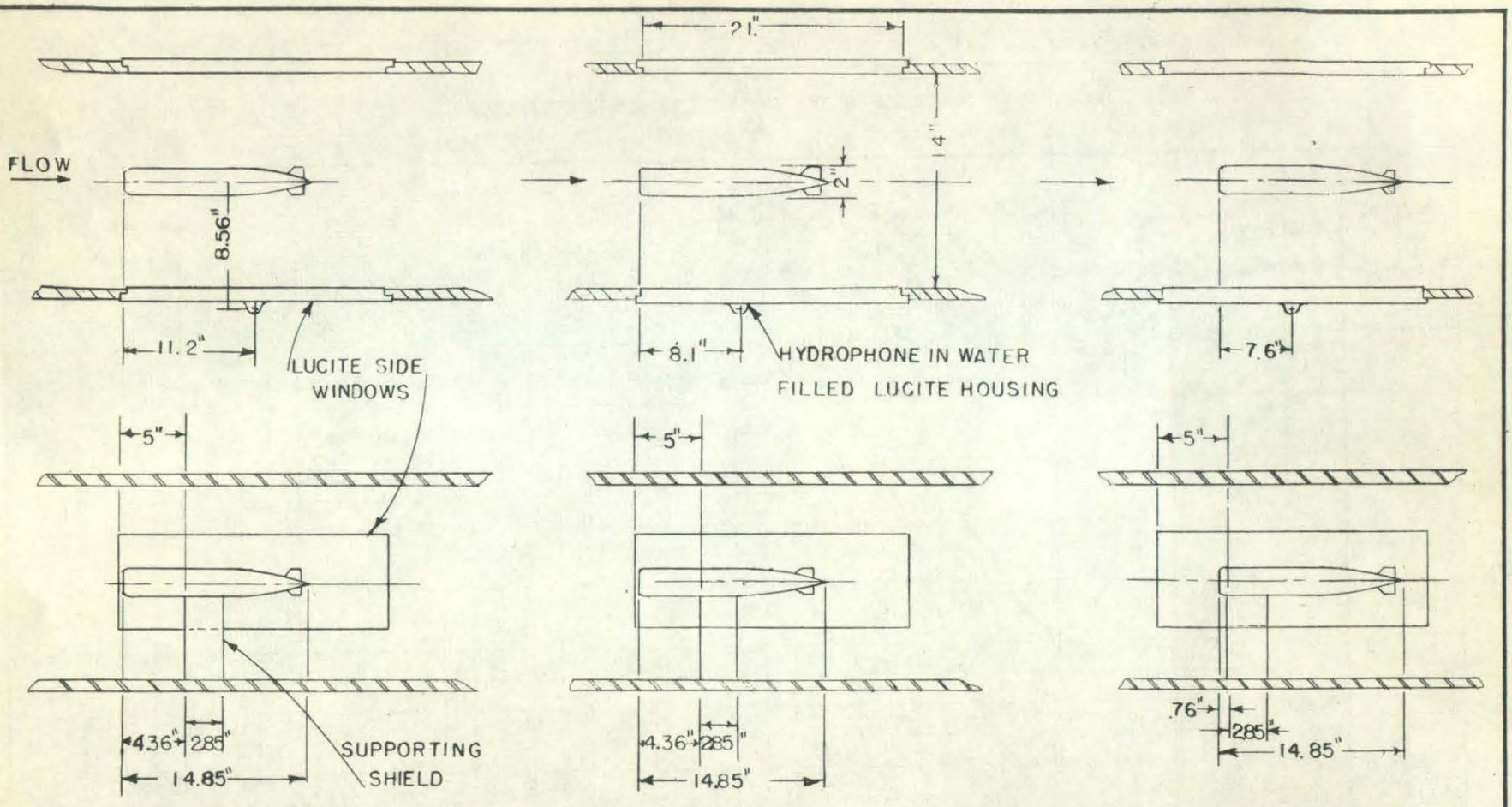

MODEL WITH TRUNCATED HEMISPHERICAL NOSE

HYDRAULIC MACHINERY LABORATORY CALIFORNIA INSTITUTE OF TECHNOLOGY PASADENA, CALIFORNIA	
RELATIVE POSITIONS OF HYDROPHONE & MODEL	
DR HCY 8-30	SCALE 1/2 = 1"
CH CME 8-31	ND 1234-U
AP H.S. 8-31	

FIG 20

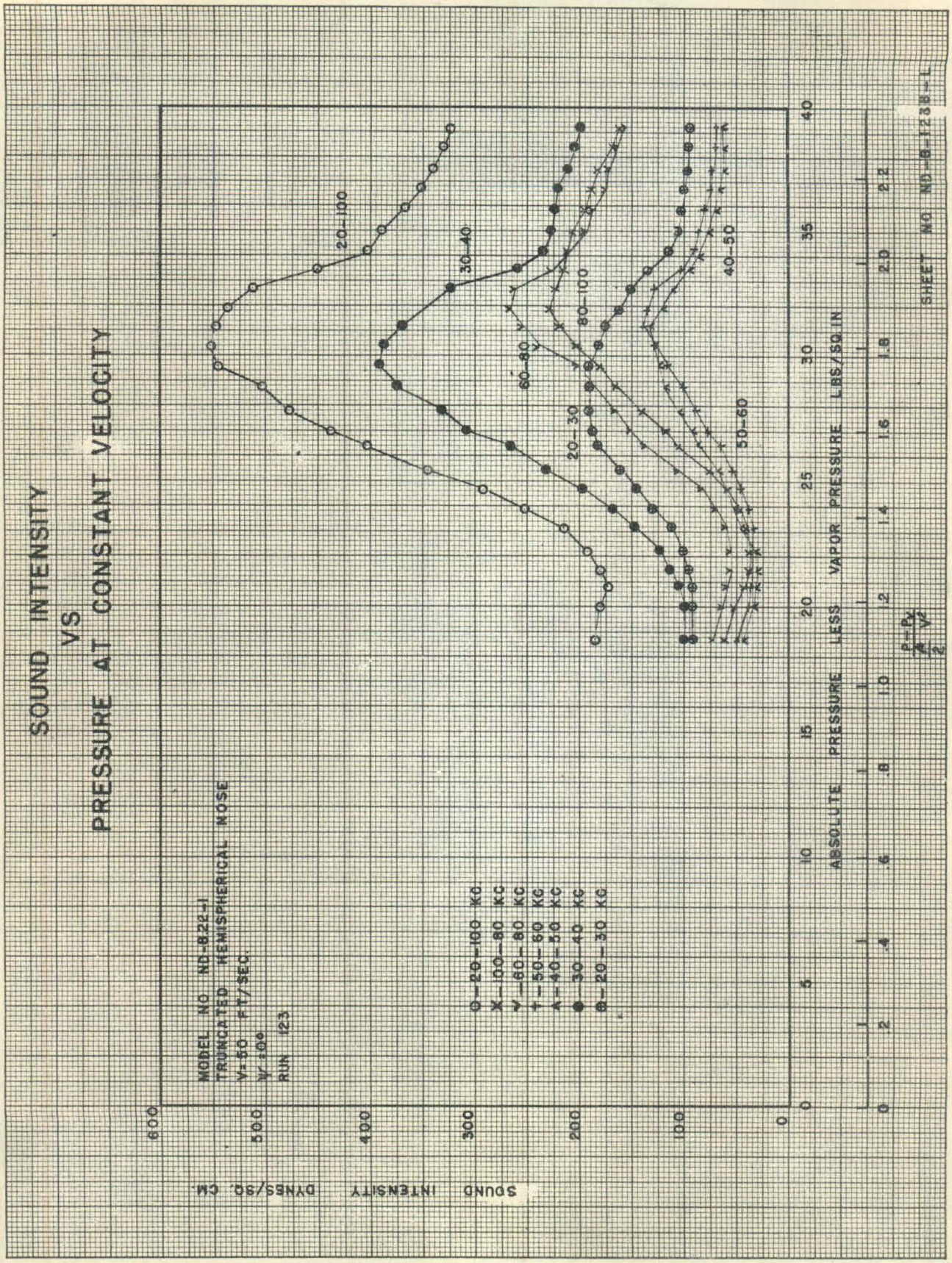
SOUND INTENSITY
VS
PRESSURE AT CONSTANT VELOCITY
MODEL NO ND-822-1
TRUNCATED HEMISPHERICAL NOSE
V=50 FT/SEC.
W=100
RUN 123
0—20—100 KC
X—100—80 KC
V—60—80 KC
+—50—60 KC
Δ—40—50 KC
●—30—40 KC
⊕—20—30 KC
SOUND INTENSITY DYNES/SQ. CM.
ABSOLUTE PRESSURE LESS VAPOR PRESSURE LBS/SQ.IN
SHEET NO ND-8-1238-L

FIG 21

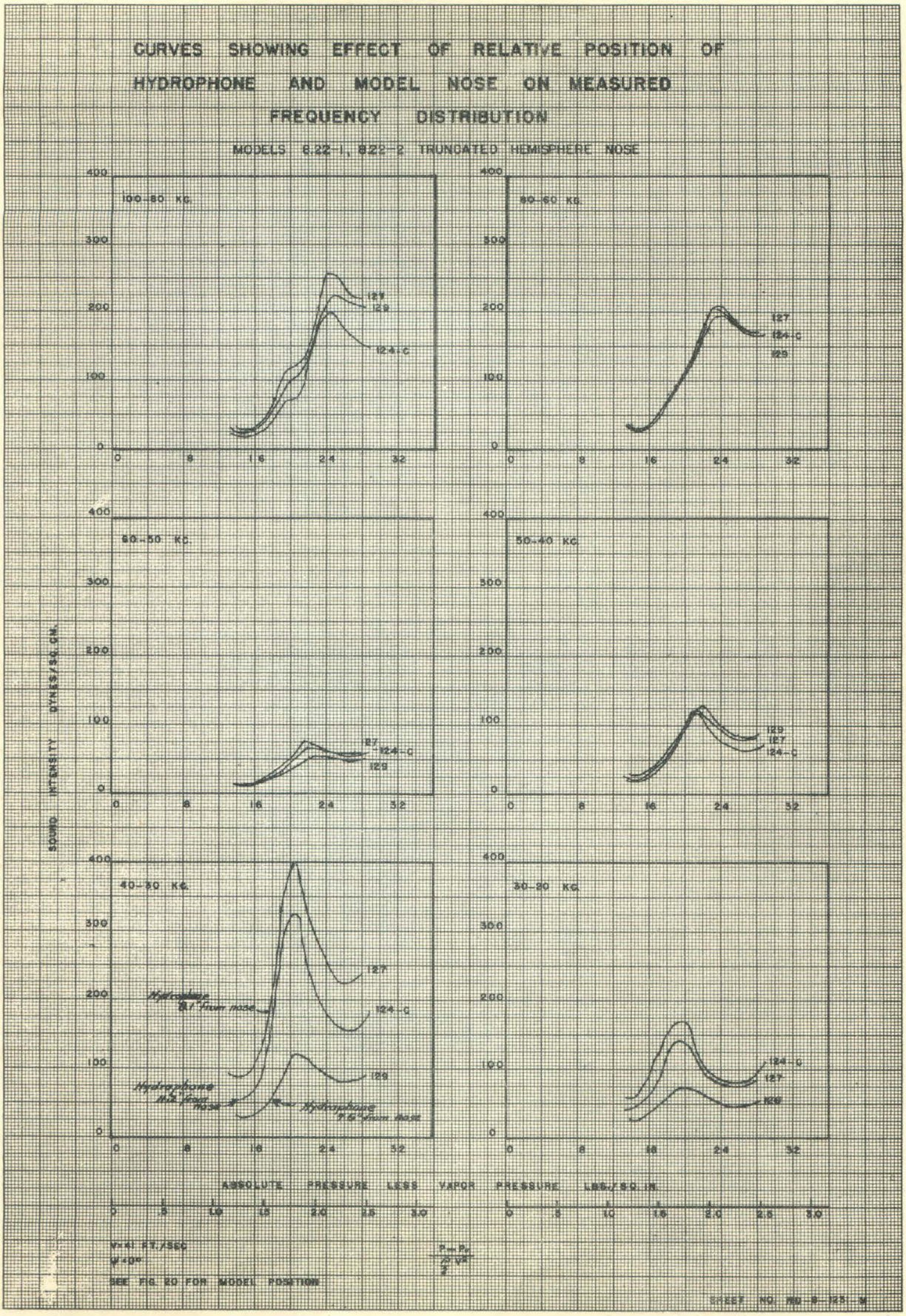
CURVES SHOWING EFFECT OF RELATIVE POSITION OF HYDROPHONE AND MODEL NOSE ON MEASURED FREQUENCY DISTRIBUTION
MODELS 822-1, 822-2 TRUNCATED HEMISPHERE NOSE
100-80 KC.
80-60 KC.
60-50 KC.
50-40 KC.
40-30 KC.
30-20 KC.
127
129
124-C
SOUND INTENSITY DYNES/SQ. CM.
Hydrophone 8.1" from nose
Hydrophone 11.2" from nose
Hydrophone 7.6" from nose
ABSOLUTE PRESSURE LESS VAPOR PRESSURE LBS./SQ. IN.
V=41 FT./SEC
ψ=0°
SEE FIG. 20 FOR MODEL POSITION
$\frac{P-P_v}{\frac{\rho}{2}V^2}$

FIG. 22

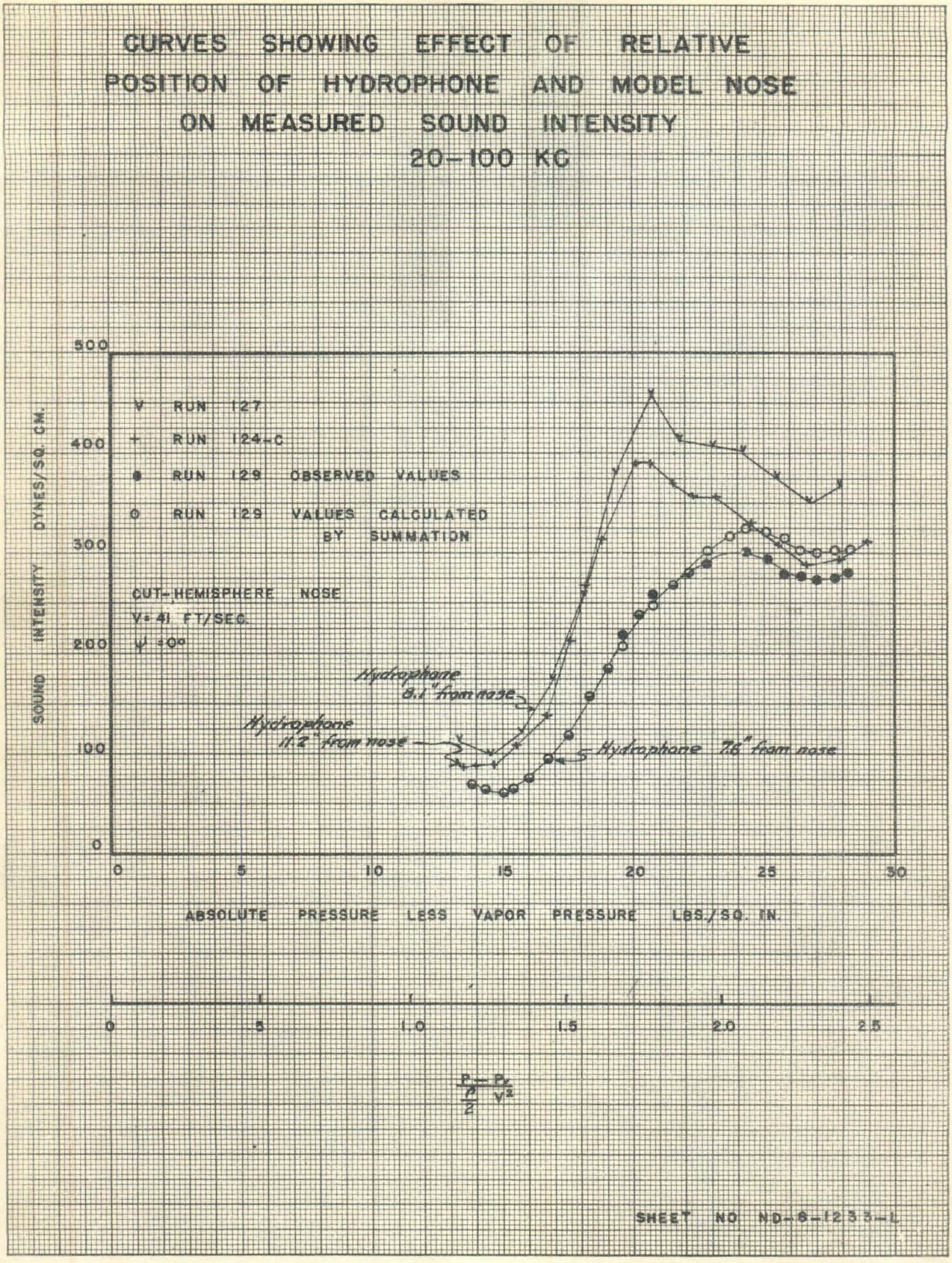
CURVES SHOWING EFFECT OF RELATIVE POSITION OF HYDROPHONE AND MODEL NOSE ON MEASURED SOUND INTENSITY 20-100 KC
SOUND INTENSITY DYNES/SQ. CM.
500
400
300
200
100
0
V RUN 127
+ RUN 124-C
● RUN 129 OBSERVED VALUES
○ RUN 129 VALUES CALCULATED BY SUMMATION
CUT-HEMISPHERE NOSE
V= 41 FT/SEC.
ψ =0°
Hydrophone 8.1" from nose
Hydrophone 11.2" from nose
Hydrophone 7.6" from nose
0
5
10
15
20
25
30
ABSOLUTE PRESSURE LESS VAPOR PRESSURE LBS./SQ. IN.
0
.5
1.0
1.5
2.0
2.5
$\frac{P-P_v}{\frac{\rho}{2}V^2}$
SHEET NO ND-8-1233-L

FIG 23

VII. THE EFFECT OF VELOCITY ON THE MEASURED SOUND INTENSITY

During the investigations it was learned that the intensity* of the sound measured during cavitation definitely increased with increasing velocity. Figures 24 and 25 show curves for tests at 31, 36, 41, and 50 feet per second with the same arrangement of projectile and hydrophone used for Run 124-C (see Figure 20). In Figure 25 are plotted the sound intensities for the total 20-100 kilocycle band against the fraction $(P-P_v)/\rho \frac{V^2}{2}$. They show how the magnitude for any value of this fraction increases with velocity. In Figure 24 the intensities measured in each frequency band are compared for the four speeds in diagrams using the same coordinates. These curves show the general trend that in each frequency band, an increase in velocity causes an increase in sound intensity for any value of $(P-P_v)/\rho \frac{V^2}{2}$. The increase in sound with increase in velocity is independent of the hydrophone and model positions. The fact that the intensity in all frequency bands increases with velocity indicates an independence of this effect from the standing wave pattern.

It would be very useful if the sound intensity varied with velocity, at constant pressure, by some simple relationship. This is not shown by the measurements in Figures 24 and 25. An investigation of the variation in the individual frequency bands, as well as in the 20-100 kilocycle range, showed no consistency between the rates of increase in intensity with increase in velocity at different values of $(P-P_v)/\rho \frac{V^2}{2}$.

The curves for the various frequency bands shown in Figure 24 indicate that the peak intensity for a given frequency band shifts to a lower value of $(P-P_v)/\rho \frac{V^2}{2}$ as the velocity is increased. Furthermore, the degree of shift increases with increasing frequency. Hence the composition of the total noise at any value of $(P-P_v)/\rho \frac{V^2}{2}$ depends on velocity. This causes the variation in shape of curves for the total 20-100 kilocycle range shown in Figure 25. Assuming the values of the fraction $(P-P_v)/\rho \frac{V^2}{2}$ are descriptive of particular degrees of cavitation as well as the beginning of cavitation, it may be inferred that the sound composition for a given stage in the development of cavitation depends on velocity.

* See footnote page 3

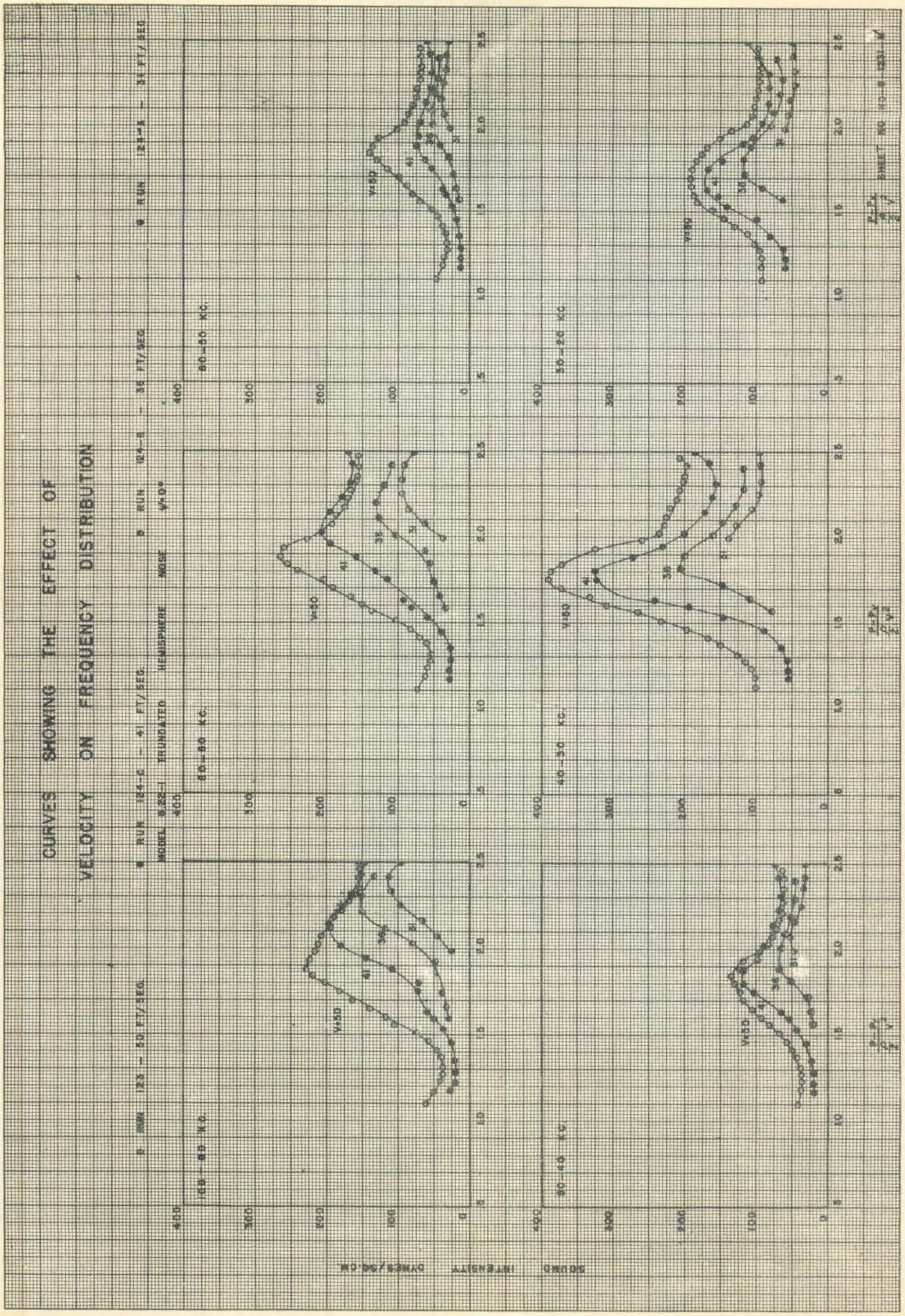
CURVES SHOWING THE EFFECT OF
VELOCITY ON FREQUENCY DISTRIBUTION
SOUND INTENSITY DYNES/SQ.CM.
90-50 KC.
50-30 KC.
80-60 KC.
40-30 KC.
100-80 KC.
50-40 KC.
V=50

FIG. 24

CURVES SHOWING EFFECT OF VELOCITY ON SOUND INTENSITY 20–100 KC

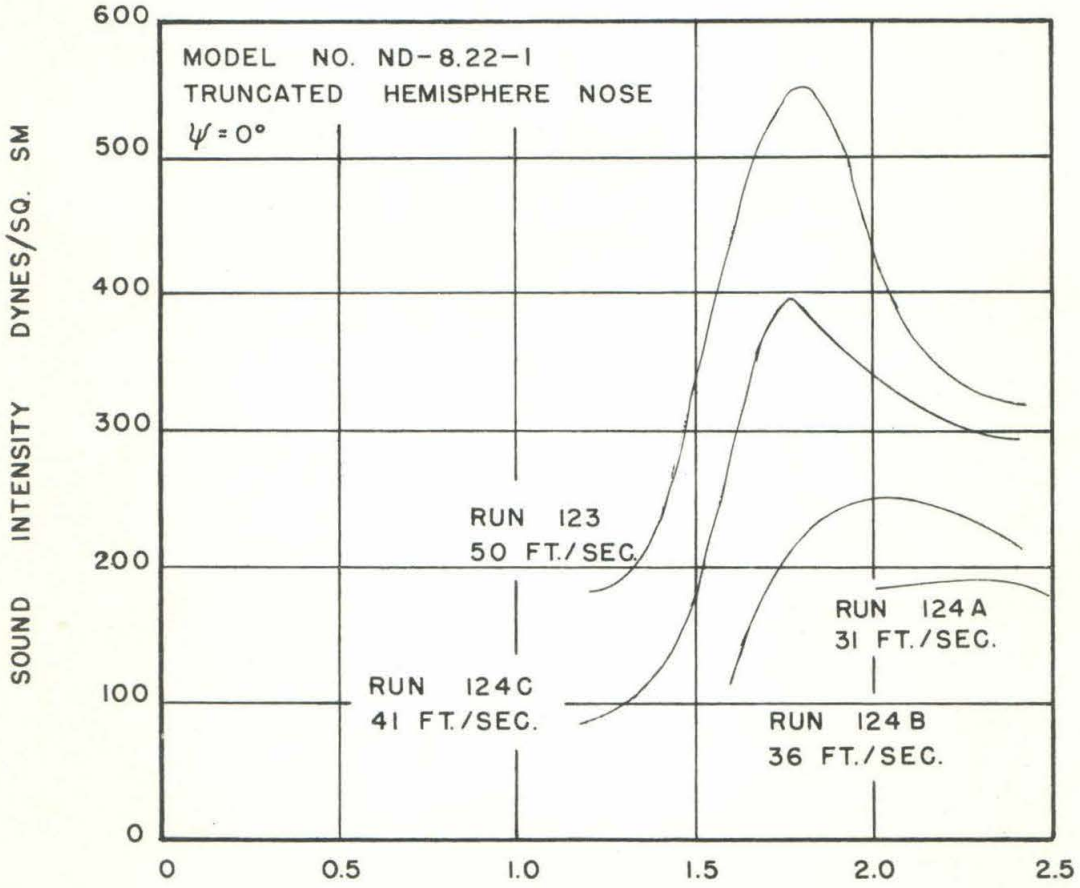

SHEET NO. ND-8-1273-L

FIG. 25

APPENDIX

I. DESCRIPTION OF SOUND MEASURING EQUIPMENT

The sound measuring equipment was designed to amplify the output of the detecting hydrophone in selected frequency ranges and to indicate the amplified voltage on a meter. The actual acoustic pressure is proportional to the voltage recorded.* A block diagram of the sound detecting and measuring apparatus is shown in Figure 4. The hydrophone output is fed through a pre-amplifier stage into the first high-gain amplifier. Low and high pass filters follow this amplifier. These filters are set to pass the band of frequencies for which measurements are being taken. The output of the filters is passed through an attenuator and a second high-gain amplifier and then to the voltmeter. Figures A-1 and A-2 show front and rear views of the completed measuring equipment together with the hydrophone and voltmeter.

The hydrophone employed in these tests is a Brush C-11-A1. Manufacturer's data supplied with the instrument state its frequency response to be flat within ± 2 decibels over a frequency range of 1 to 100 kilocycles, and its operation to be linear over a pressure range of 2 to 50,000 dynes per square centimeter. It is stated that there is no directional effect below 50 kilocycles, and that above 50 kilocycles maximum response is obtained when the plane of the diaphragms is perpendicular to the plane of the oncoming wave front. Most uniform frequency response is said to be obtained with the hydrophone in this position. Photographs of the hydrophone are shown in Figures A-3A and A-3B. The instrument was checked in the Laboratory by applying a voltage of known amplitude and frequency in series with the crystal, and its response was found to be better than stated by the manufacturer. Both the manufacturer's response curve and the curve obtained in the laboratory are shown in Figure A-9. The circuit diagram of the hydrophone is shown in Figure A-5.

The input amplifier isolates the hydrophone from the rest of the equipment. It consists of a 1R5 tube used a a completely degenerative triode. The wiring diagram of the unit is shown in Figure A-5. There it is seen that three possible terminating resistances are provided to match other hydrophone preamplifiers that may be used. Provision was made for installing a high pass filter between the hydrophone output and the first amplifier input in case the level of the low frequency noise picked up by the hydrophone was so large compared to the high frequency noise that the first amplifier might be overloaded. Experiments showed this to be unnecessary and the filter unit was not employed. The response curve for this amplifier unit with the filter out is shown in Figure A-10. It may be seen that the response of this unit is constant within ± 0.5 decibels over the frequency range 1-100 kilocycles.

* See footnote page 3

The amplifier units are of conventional resistance coupled design. The last stage of each is a 6AC7 pentode tube used as a cathode follower to provide isolation and allow the amplifiers to feed a low impedance (600) line. The 50 decibel gain amplifier uses a pair of 6AC7 pentode tubes in cascade before the cathode follower, and the 40 decibel amplifier uses a pair of 6SJ7 pentode tubes in cascade before the cathode follower. The wiring diagrams of these units are shown in Figure A-6 and the response curves in Figure A-11. Examination of the curves shows the frequency response of each amplifier to be flat within ± .5 decibels over the frequency range 1-100 kilocycles.

The filters consist of 3 cascaded T sections, one prototype secgion, one M derived sharp cutoff section with M = 0.25, and one sharp cutoff M derived section with M = 0.5 which is transformed into a π section, split, and used as the terminating half sections. The wiring diagrams of the filter units are shown in Figure A-7. Each filter may be set individually for a cutoff frequency of 1, 5, 10, 20, 30, 40, 50, 60, 80, or 100 kilocycles. The response curves for the filter units in cascade and used as a band pass filter are shown for various bands in Figures A-13 to A-17. These curves show that in each case the secondary peaks outside the pass band are at least 20 decibels lower than the pass band itself. Twenty decibels represents a voltage ratio of 10 to 1.

The attenuator unit consists of two 600 ohm T pads. One pad has a range of 10 decibels and is adjustable in 1 decibel steps. The other has a range of 100 decibels and is adjustable in 10 decibel steps. The wiring diagram of this unit is shown in Figure A-8. The response curves, Figure A-12, show the attenuator unit to have a loss as read on the pads ± .5 decibels at any attenuation setting less than 40 decibels over a frequency range of 1-100 kilocycles. The combination of this unit and amplfiers #1 and #2 can be used to give any amplification between 0 and 90 decibels in one decibel steps.

The oscillator used is a Hewlett-Packard Model #200-CR. This instrument is stated by the manufacturers to be flat within 1 decibel over a frequency range of 1 to 100 kilocycles. The vacuum tube voltmeter used is a Hewlett Packard Model #400-A. This instrument is stated by the manufacturers to be flat within ± 1 decibel over a frequency range of 1 to 100 kilocycles. This meter is designed to read the average full wave value of the voltage being measured.

The amplifier units are connected to a common power supply. The wiring diagram of this unit is shown in Figure A-8.

II. OPERATION OF SOUND MEASURING EQUIPMENT

It is shown in the wiring diagrams that the input and output impedance of each unit is 600 ohms. This feature allows the units to be connected in any sequence that is desired. Furthermore, the voltmeter, which has a high impedance input, may be used to measure the voltage at the junction between any two units without disturbing the operation of the measuring equipment. In practice, the equipment is set in operation and the voltage read at the input of each unit. If the voltage at the input of an amplifier were so high as to cause overloading and consequent errors in measurements, the sequence of the units could be changed to correct this condition. In all measurements taken to date the sequence shown in the block diagram, Figure 4, has been used. With this setup the voltage corresponding to the maximum sound intensity encountered is approximately 1.5 volts with the attenuator unit set to give about 20 decibels attenuation.

The output voltage of the hydrophone itself was measured under various conditions of tunnel operation to determine if low frequency noise from the pumps might be overloading the hydrophone. It was found in all cases that the total noise picked up by the hydrophone was less than 20% of the amount necessary to cause the operation of the instrument to be non-linear.

It was found necessary to allow the equipment to warm up for about 15 minutes to eliminate errors due to the gain of the amplifiers shifting before thermal equilibrium became established.

III. CALIBRATION OF EQUIPMENT AND CALCULATION OF RESULTS

To convert the voltages measured to their equivalents in dynes/sq cm acoustic pressure, it is necessary to know the constant which relates the acoustic pressure reaching the hydrophone to the voltage output of the instrument.* The Brush Development Company states in their report No. LR-47 that the sensitivity of the C-11-A1 hydrophone, expressed in terms of voltage across the calibrating resistor is, except for a small temperature correction, .012 millivolts/dynes/sq cm. This temperature correction is denoted by the symbol C_T. The value of C_T varies from 1.16 at 55° F to 1.00 at 78° F. The pressure reaching the hydrophone may be determined by noting the hydrophone output in the presence of the sound, noting the voltage across the calibration resistor which will produce the same output in the absence of the sound, and dividing this voltage, expressed in millivolts, by .012 and multiplying by the temperature correction figure C_T. As is shown in Figure A-5, the circuit diagram of the preamplifier, there is a 1000 ohm resistor between the hydrophone calibration resistor and the calibration input terminals. Hence the voltage at the calibrating terminals in volts is equal to the

* See footnote page 3

the voltage across the calibrating resistor in millivolts. In practice the voltage at the input terminals which will cause an output voltage of 1 volt is measured. This voltage is denoted by the symbol V_o. This is done with the filters out, or set at O and infinity. Hence the acoustic pressure which causes an output voltage L, may be calculated by the formula:

$$I = \frac{V_o C_T L}{.012}$$

The frequency response curves of the filter units, Figure 13-A to Figure 17-A, show that there is attenuation in the pass band. Furthermore, the degree of attenuation is different for each filter configuration. To correct for this, a filter correction constant (K_F) has been calculated for each filter setup. The values of K_F were calculated to correct for the attenuation of the filters if a signal of uniform frequency distribution having the same frequency range as the pass band of the filters was impressed on the equipment. This was done by measuring the ratio of output voltage to input voltage within the pass band. The square of this ratio was plotted to a linear frequency base. The square root of the ratio of the area under the curve so plotted to the area of the total plot was taken and its reciprocal called K_F. The values of K_F vary from 1.160 for the frequency band 20 to 100 kilocycles to 1.876 for the 80 to 100 kilocycle band. The sound pressure within a given frequency band is calculated by the formula

$$I = \frac{V_o C_T K_F L}{.012}$$

where

I = acoustic pressure in dynes/cm^2

C_T = temperature correction constant for temperature of hydrophone

K_F = filter correction constant for pass band used

L = measured output voltage

V_o = volts across calibrating terminal which will produce 1 volt output with filters set at O and infinity

IV. HYDRAULIC PRESSURE CONTROL SYSTEM

The establishing and maintaining of steady cavitation conditions require that the hydraulic pressure in the Water Tunnel working section be held constant within very close limits. The

system of pressure control used is that described in the memorandum of Reference 1. This system, which is shown in bold relief in the isometric diagram, Figure A-18, is composed of a pressure-regulating circuit pump which supplies water at a given pressure through the horizontal line, and the regulating circuit throttle valve at the large stilling tank. Since the system is closed except for this auxiliary pressure circuit, provision must be made for discharging the same amount of water as is supplied by the pressure-regulating pump. This discharge flows through the "by-pass" valve and is returned to the supply pump. The pressure in the stilling tank varies with the amount of opening of the by-pass valve and of the regulating circuit throttle valve. When the by-pass valve is nearly closed, the maximum pressure is developed in the system. When the by-pass valve is wide open, a low pressure is maintained in the system which can be decreased further by operating a pump in the by-pass line (not shown), or by throttling with the throttle valve in the supply line of the circuit. In controlling the pressure for the cavitation runs, both the by-pass and the throttle valves were used.

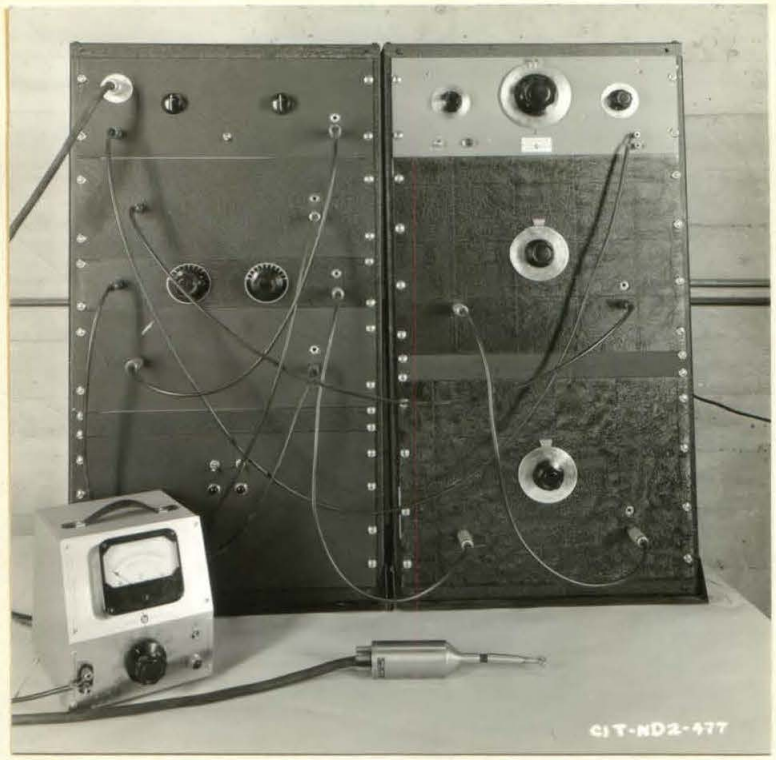

FIGURE A–1

FRONT VIEW OF HYDROPHONE, ELECTRONIC VOLTMETER, AND RACKED EQUIPMENT. THE UNITS ARE CONNECTED FOR USE IN THIS PHOTOGRAPH.

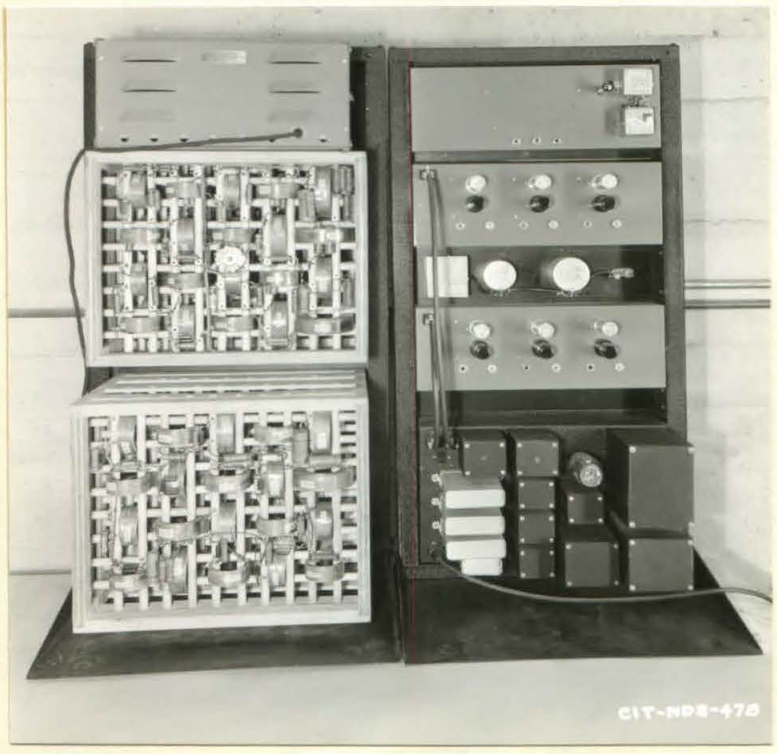

FIGURE A–2

BACK OF RACKED EQUIPMENT. NOTE METHOD OF MOUNTING FILTER COILS.

VIEW OF INSTALLATION OF SOUND DETECTING AND MEASURING EQUIPMENT.

FIGURE A-3A

FIGURE A-3B

DETAILS OF HYDROPHONE AND LUCITE MOUNTING BLISTER

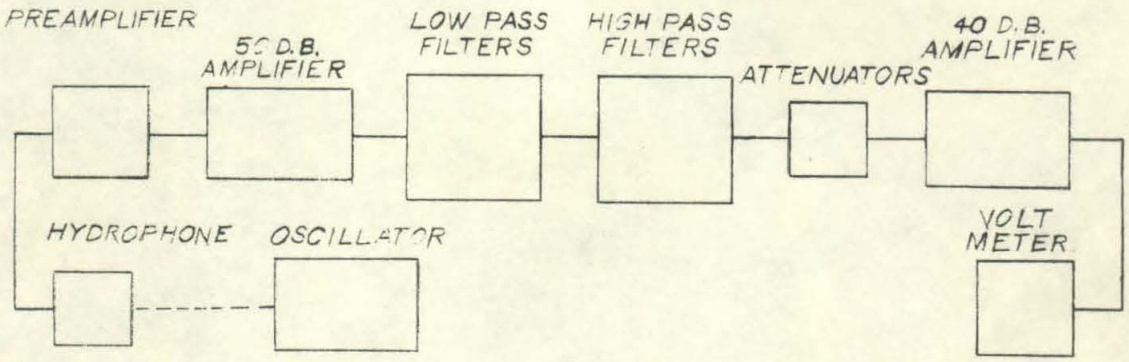

HYDRAULIC MACHINERY LABORATORY CALIFORNIA INSTITUTE OF TECHNOLOGY		
DR C.M.E. CH H. S. AP	BLOCK DIAGRAM OF SOUND DETECTING AND MEASURING EQUIPMENT	SCALE ND-1221-L

FIG. 4

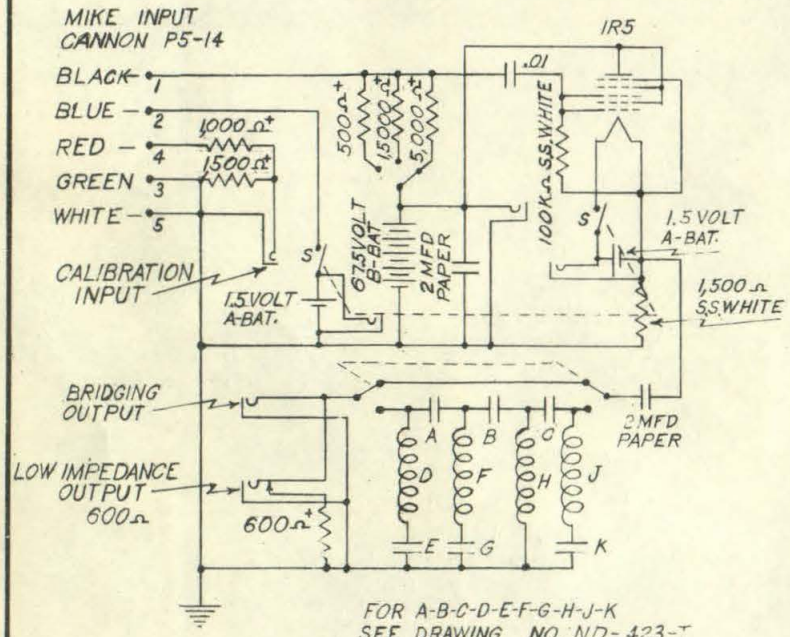

FOR A-B-C-D-E-F-G-H-J-K
SEE DRAWING NO. ND-423-T

+DAVEN TYPE B.W.T.
NON INDUCTIVE RESISTORS

HYDRAULIC MACHINERY LABORATORY	CALIFORNIA INSTITUTE OF TECHNOLOGY	
DR C.M.E. 6-10-43 CH H.S. 6-10-43 AP	SOUND SURVEY PREAMP	SCALE ND-422 -T

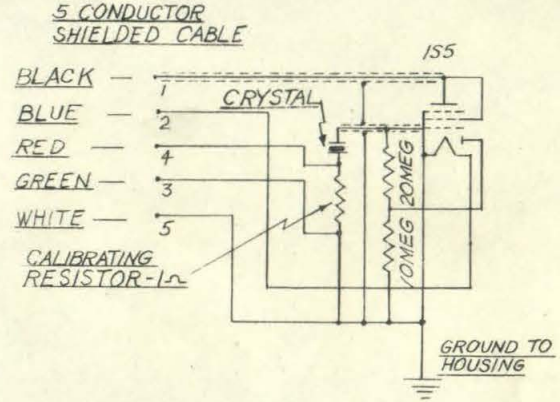

TAKEN FROM CONFIDENTIAL REPORT NO. LR-47
PAGE 14 BY BRUSH DEVELOPMENT CO.

HYDRAULIC MACHINERY LABORATORY	CALIFORNIA INSTITUTE OF TECHNOLOGY	
DR CME CH HS AP	SOUND SURVEY BRUSH *C-11-A1 HYDROPHONE	SCALE ND-424 -T

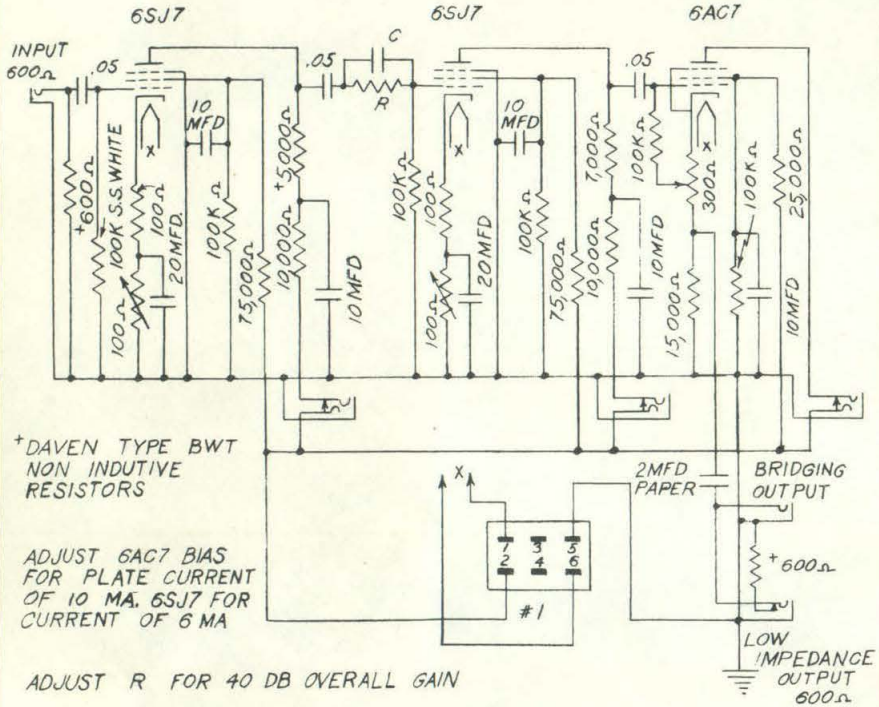

HYDRAULIC MACHINERY LABORATORY CALIFORNIA INSTITUTE OF TECHNOLOGY		
DR C.M.E. 6-12-43 CH H.S. AP	SOUND SURVEY 40 DB. AMPLIFIER	SCALE ND-426 -T

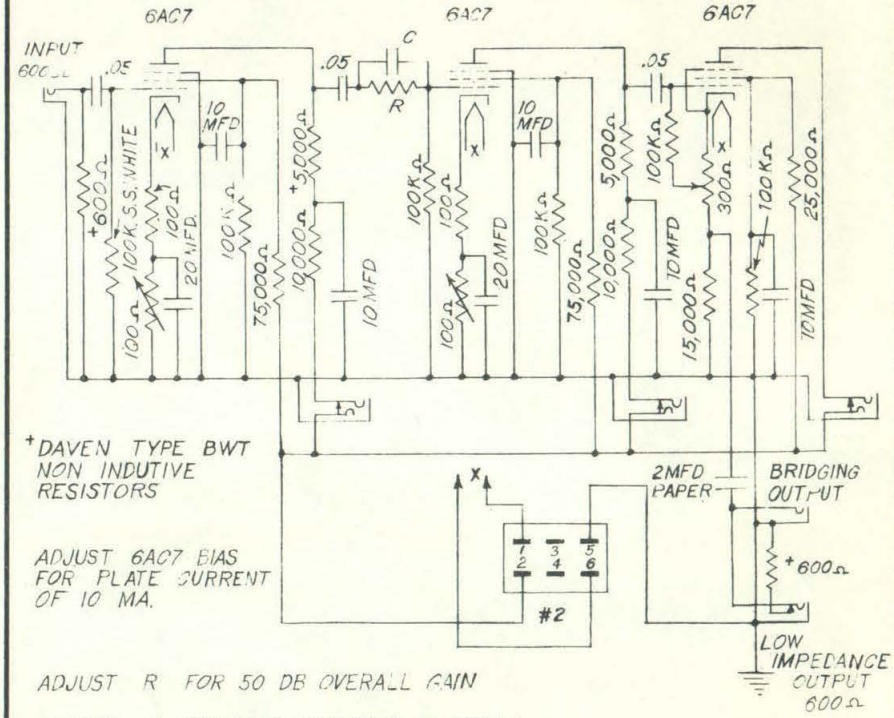

HYDRAULIC MACHINERY LABORATORY CALIFORNIA INSTITUTE OF TECHNOLOGY		
DR C.M.E. 6-11-43 CH H.S. AP	SOUND SURVEY 50 DB. AMPLIFIER	SCALE ND-425 -T

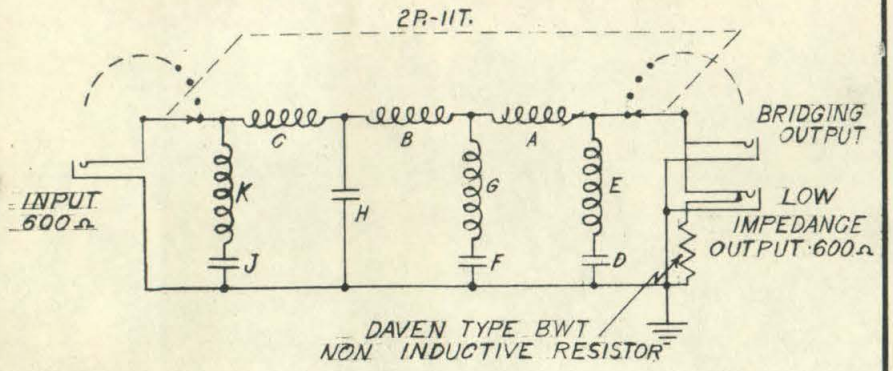

CUT OFF KC.	A mh.	B mh.	C,E,K, mh.	G mh.	D,F,J mfd.	H mfd.
1	71.6	119.0	143.0	179.0	.133	.531
5	14.3	23.9	28.6	35.8	.0265	.106
10	7.16	11.9	14.3	17.9	.0133	.0531
20	3.58	5.97	7.16	8.95	.00663	.0265
30	2.39	3.98	4.78	5.97	.00443	.0177
40	1.79	2.98	3.58	4.47	.00333	.0133
50	1.43	2.39	2.86	3.58	.00265	.0106
60	1.19	1.99	2.39	2.98	.00221	.00884
80	.896	1.49	1.79	2.24	.00166	.00663
100	.716	1.19	1.43	1.79	.00133	.00531

HYDRAULIC MACHINERY LABORATORY CALIFORNIA INSTITUTE OF TECHNOLOGY

DR C.M.E. | CH H.S. | AP

SOUND SURVEY
LOW PASS FILTERS

SCALE
ND-431 -T

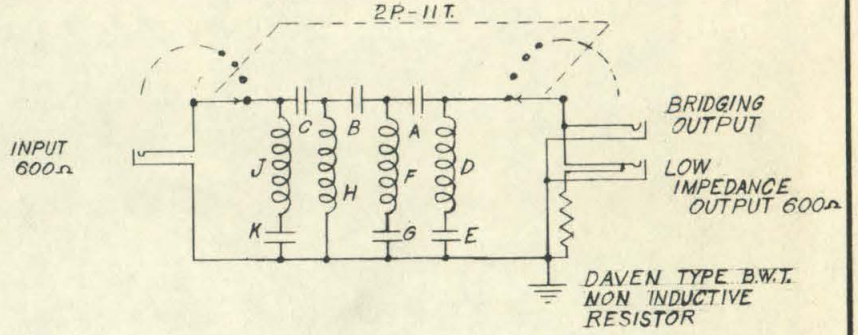

CUT OFF KC.	A mfd.	B mfd.	C,E,K, mfd.	G mfd.	D,F,J, mh.	H mh.
1	.355	.213	.177	.142	191.	47.8
5	.0706	.0424	.0353	.0282	38.2	9.55
10	.0355	.0213	.0177	.0142	19.1	4.78
20	.0236	.0106	.00884	.00707	9.56	2.39
30	.0118	.00707	.00589	.00471	6.36	1.59
40	.00885	.00531	.00443	.00354	4.76	1.19
50	.00706	.00424	.00353	.00282	3.82	.955
60	.00589	.00354	.00295	.00236	3.18	.796
80	.00443	.00266	.00221	.00177	2.39	.597
100	.00355	.00213	.00177	.00142	1.91	.478

HYDRAULIC MACHINERY LABORATORY CALIFORNIA INSTITUTE OF TECHNOLOGY

DR C.M.E. 6-16-43 | CH H.S. | AP

SOUND SURVEY
HIGH PASS FILTERS

SCALE
ND-423 -T

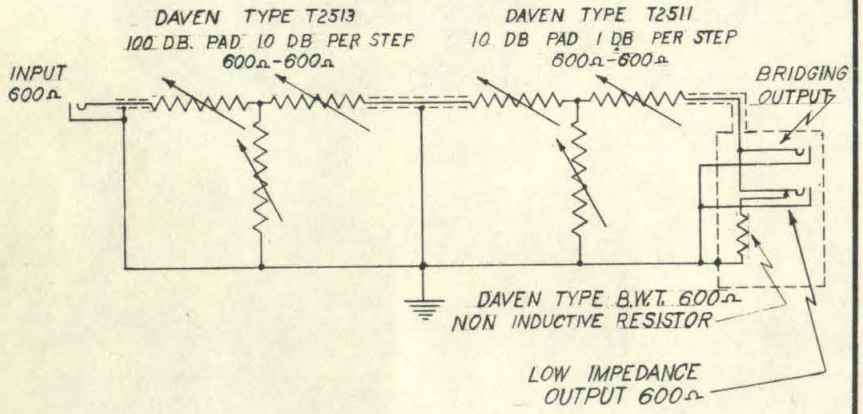

HYDRAULIC MACHINERY LABORATORY	CALIFORNIA INSTITUTE OF TECHNOLOGY	
DR C.M.E 6-14-43 CH H.S. AP	SOUND SURVEY ATTENUATORS	SCALE ND-429 -T

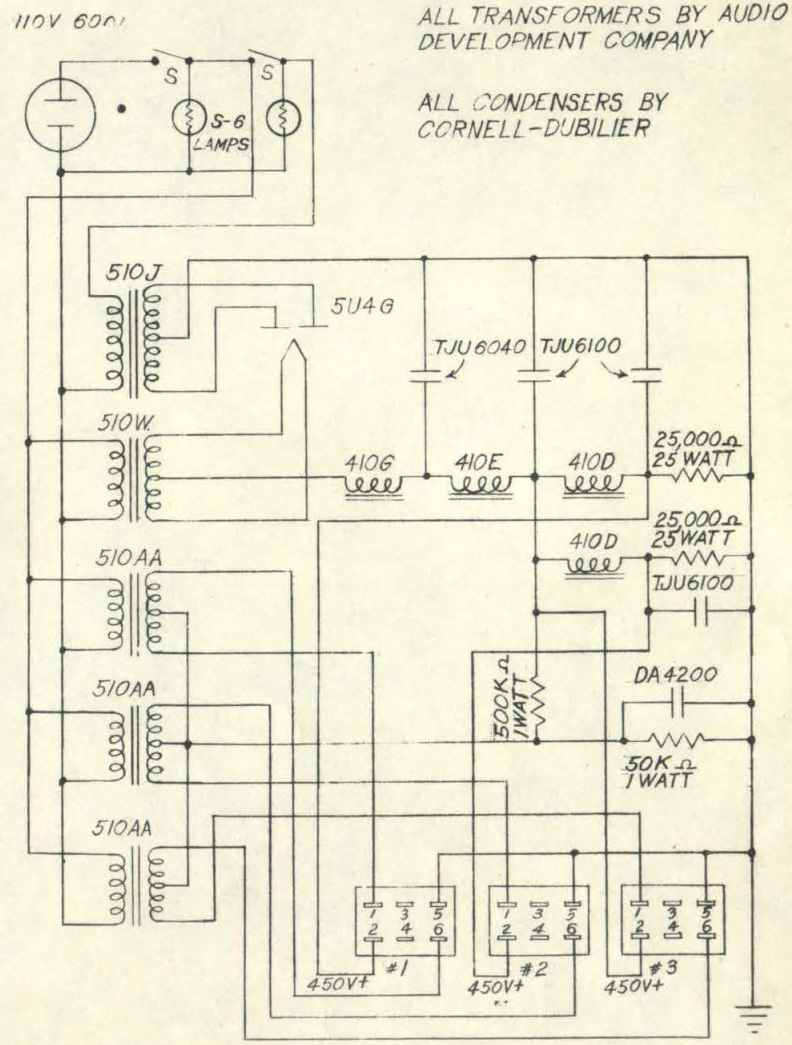

HYDRAULIC MACHINERY LABORATORY	CALIFORNIA INSTITUTE OF TECHNOLOGY	
DR C.M.E 6-7-43 CH H.S. AP	SOUND SURVEY POWER SUPPLY	SCALE ND-416 -T

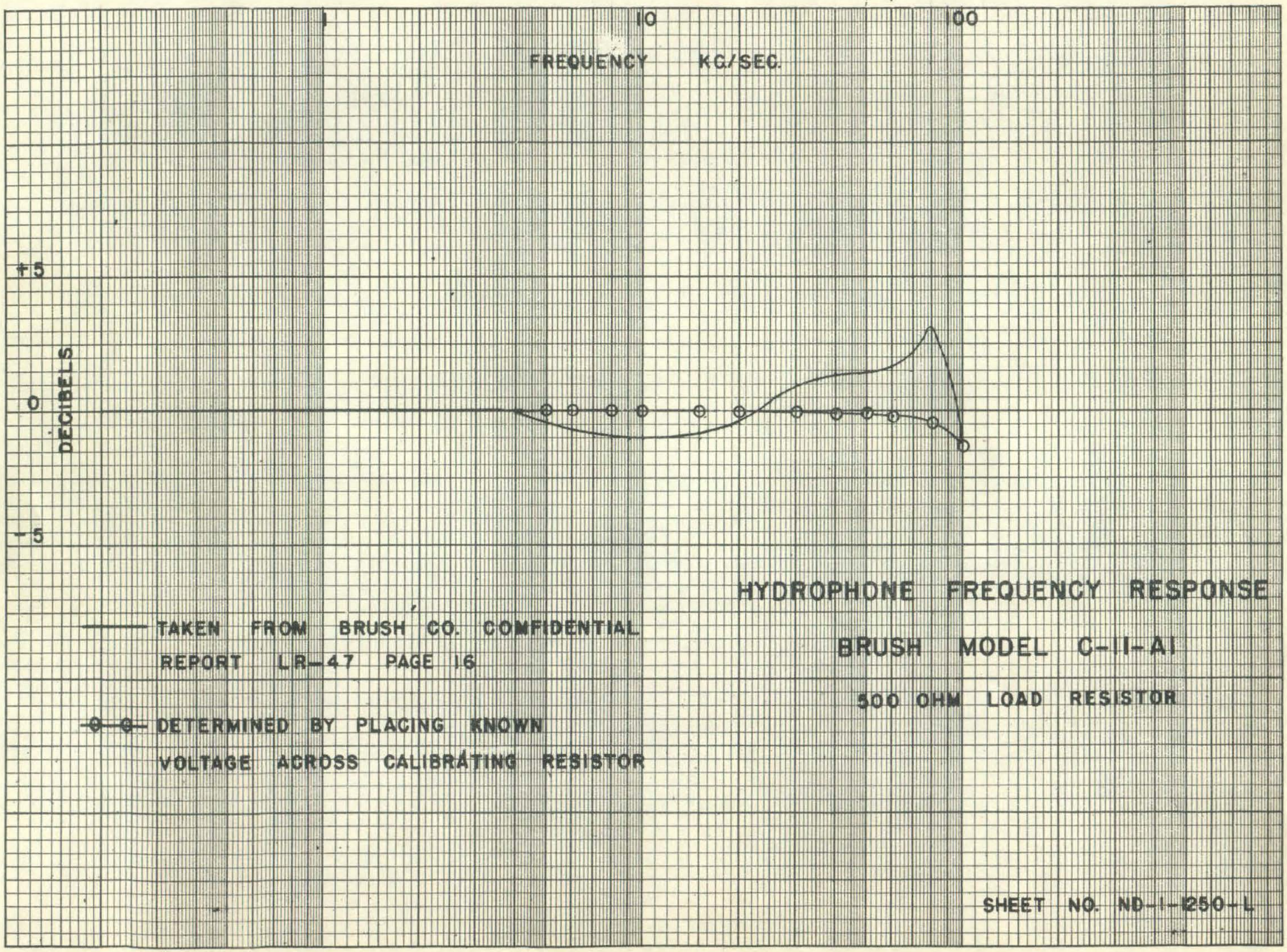
1
10
100
FREQUENCY KC./SEC.
+5
0
-5
DECIBELS
HYDROPHONE FREQUENCY RESPONSE
BRUSH MODEL C-II-AI
500 OHM LOAD RESISTOR
TAKEN FROM BRUSH CO. COMFIDENTIAL REPORT LR-47 PAGE 16
DETERMINED BY PLACING KNOWN VOLTAGE ACROSS CALIBRATING RESISTOR
SHEET NO. ND-1-250-L

FIG A-9

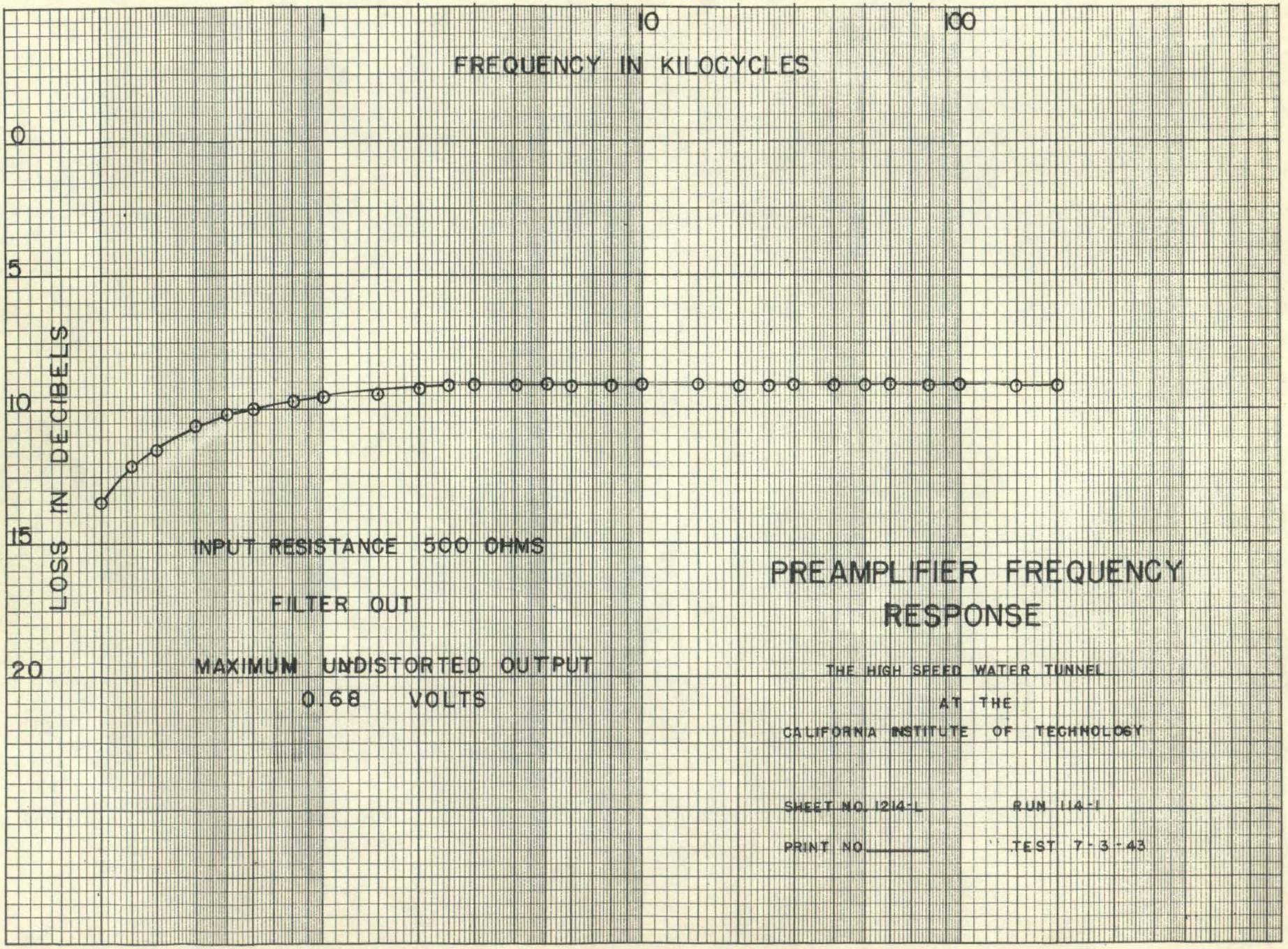
1
10
100
FREQUENCY IN KILOCYCLES
0
5
10
15
20
LOSS IN DECIBELS
INPUT RESISTANCE 500 OHMS
FILTER OUT
MAXIMUM UNDISTORTED OUTPUT
0.68 VOLTS
PREAMPLIFIER FREQUENCY RESPONSE
THE HIGH SPEED WATER TUNNEL
AT THE
CALIFORNIA INSTITUTE OF TECHNOLOGY
SHEET NO. 1214-L
RUN 114-1
PRINT NO.
TEST 7-3-43

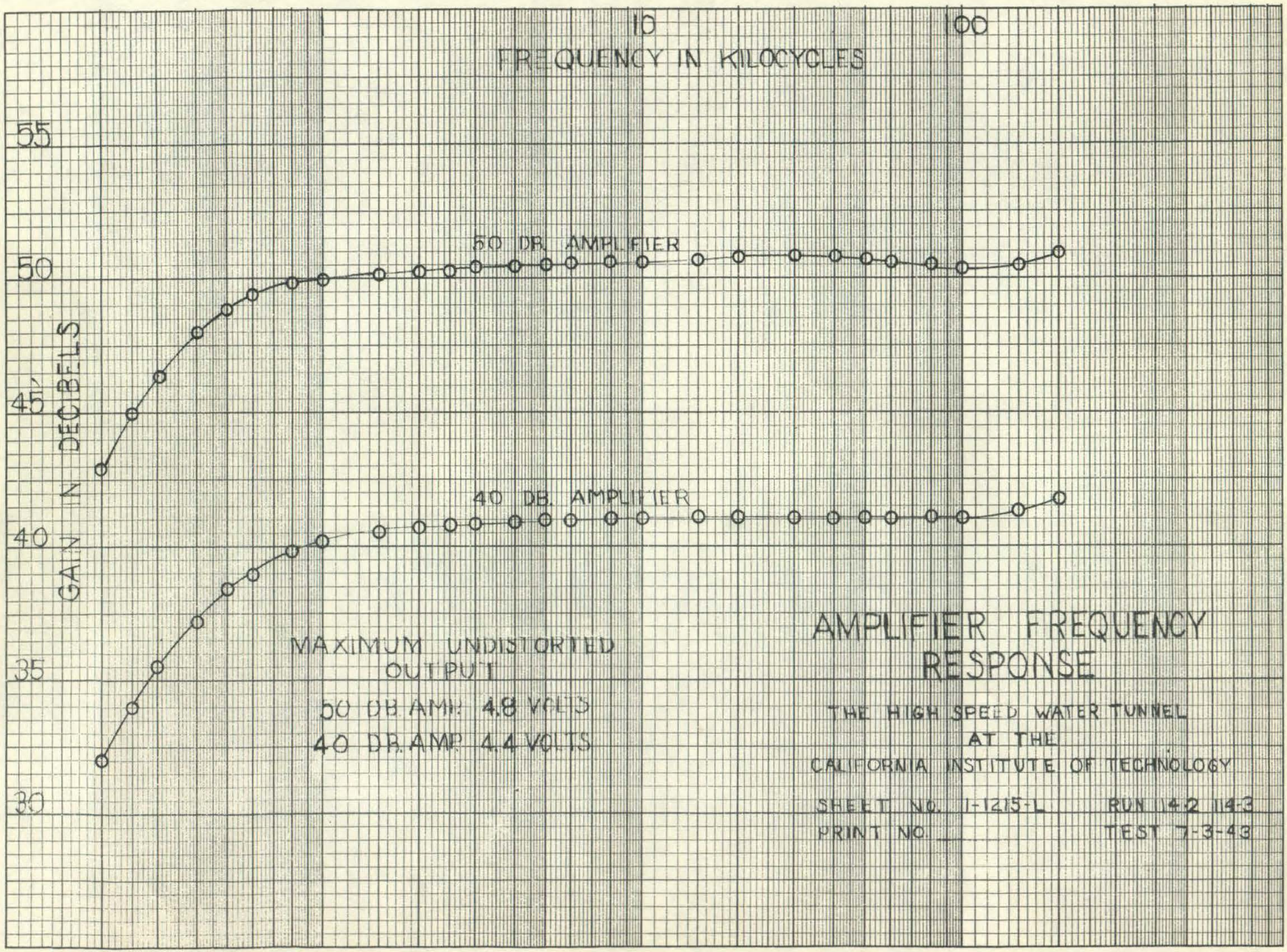
10
100
FREQUENCY IN KILOCYCLES
55
50
45
40
35
30
GAIN IN DECIBELS
50 DB. AMPLIFIER
40 DB. AMPLIFIER
MAXIMUM UNDISTORTED OUTPUT
50 DB AMP. 4.8 VOLTS
40 DB AMP. 4.4 VOLTS
AMPLIFIER FREQUENCY RESPONSE
THE HIGH SPEED WATER TUNNEL
AT THE
CALIFORNIA INSTITUTE OF TECHNOLOGY
SHEET NO. 1-1215-L
RUN 14-2 14-3
PRINT NO.
TEST 7-3-43

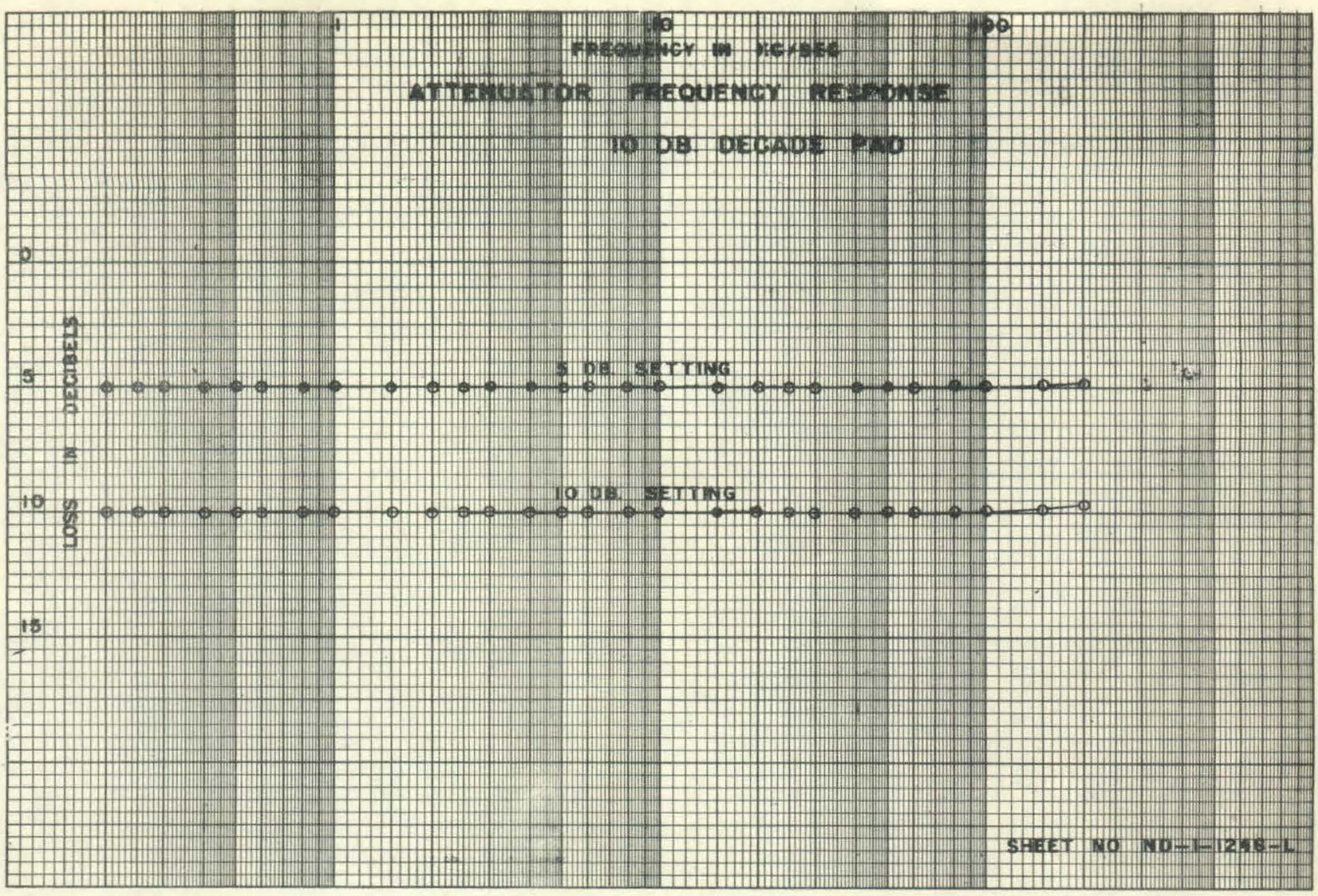
1
10
100
FREQUENCY IN KC/SEC
ATTENUATOR FREQUENCY RESPONSE
10 DB DECADE PAD
0
5
10
15
LOSS IN DECIBELS
5 DB SETTING
10 DB SETTING
SHEET NO ND-1-1248-L

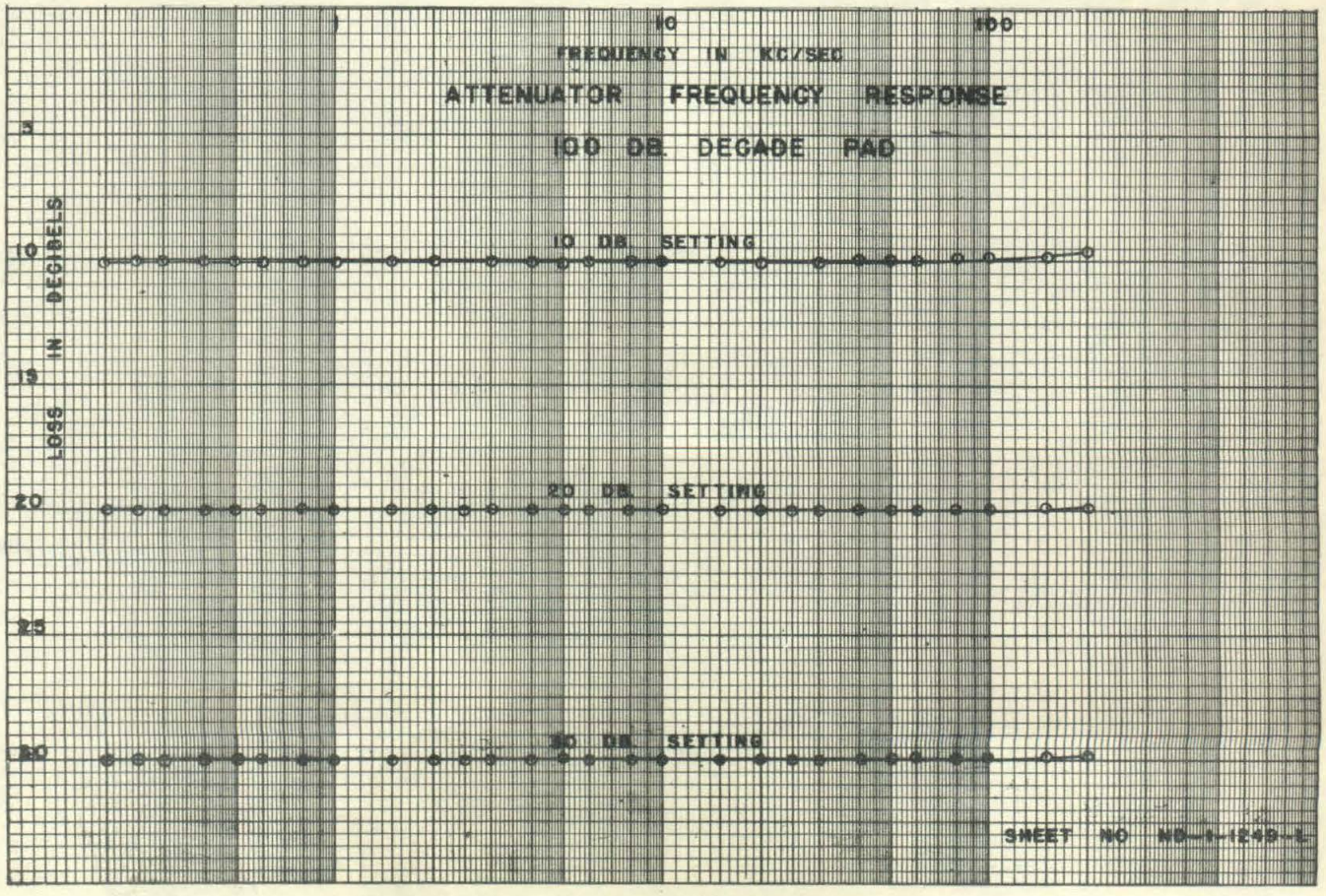
1
10
100
FREQUENCY IN KC/SEC
ATTENUATOR FREQUENCY RESPONSE
100 DB DECADE PAD
5
10
15
20
25
30
LOSS IN DECIBELS
10 DB SETTING
20 DB SETTING
30 DB SETTING
SHEET NO ND-1-1249-L

FIG A-12

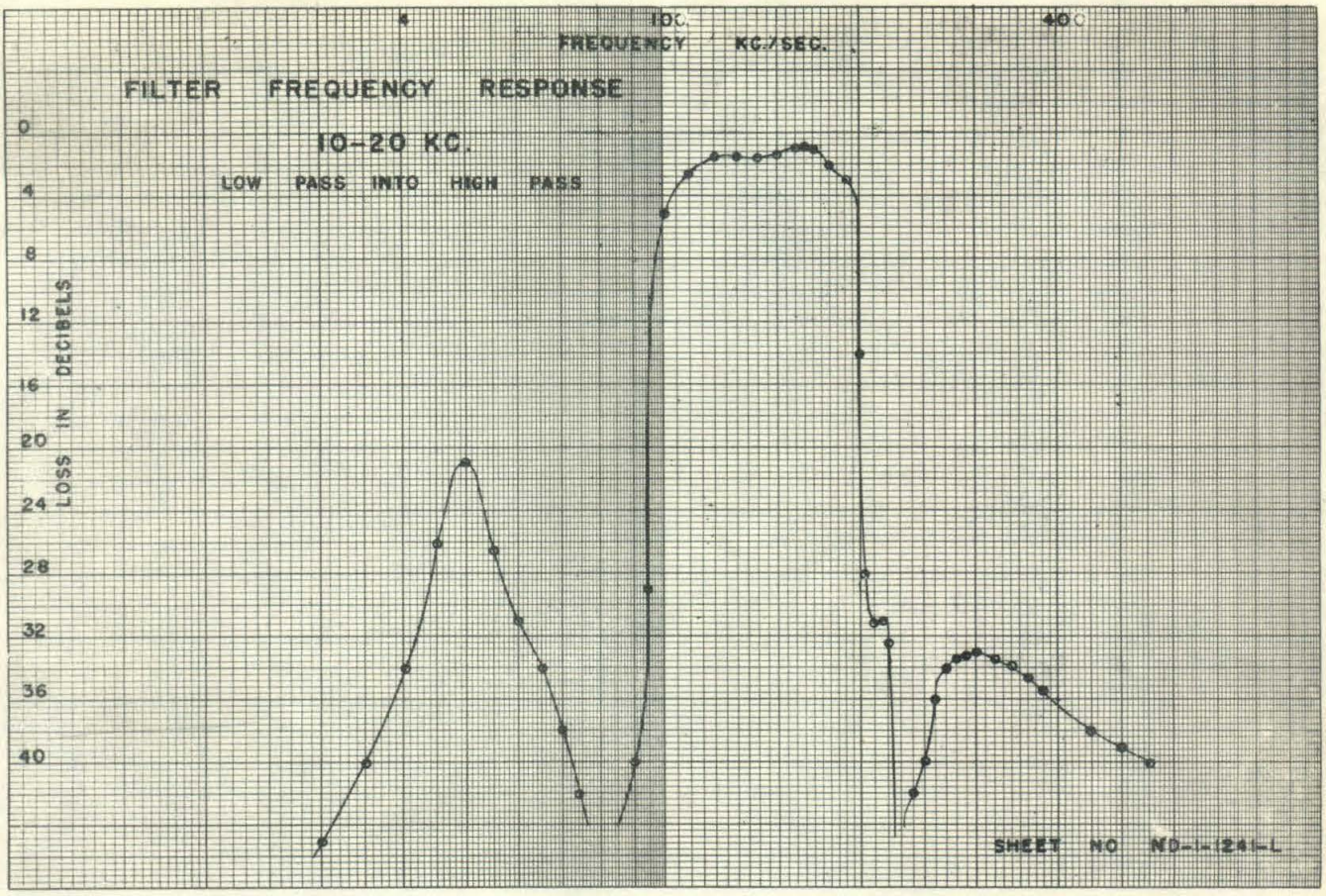
4
10
40
FREQUENCY KC./SEC.
FILTER FREQUENCY RESPONSE
10-20 KC.
LOW PASS INTO HIGH PASS
0
4
8
12
16
20
24
28
32
36
40
LOSS IN DECIBELS
SHEET NO ND-1-1241-L

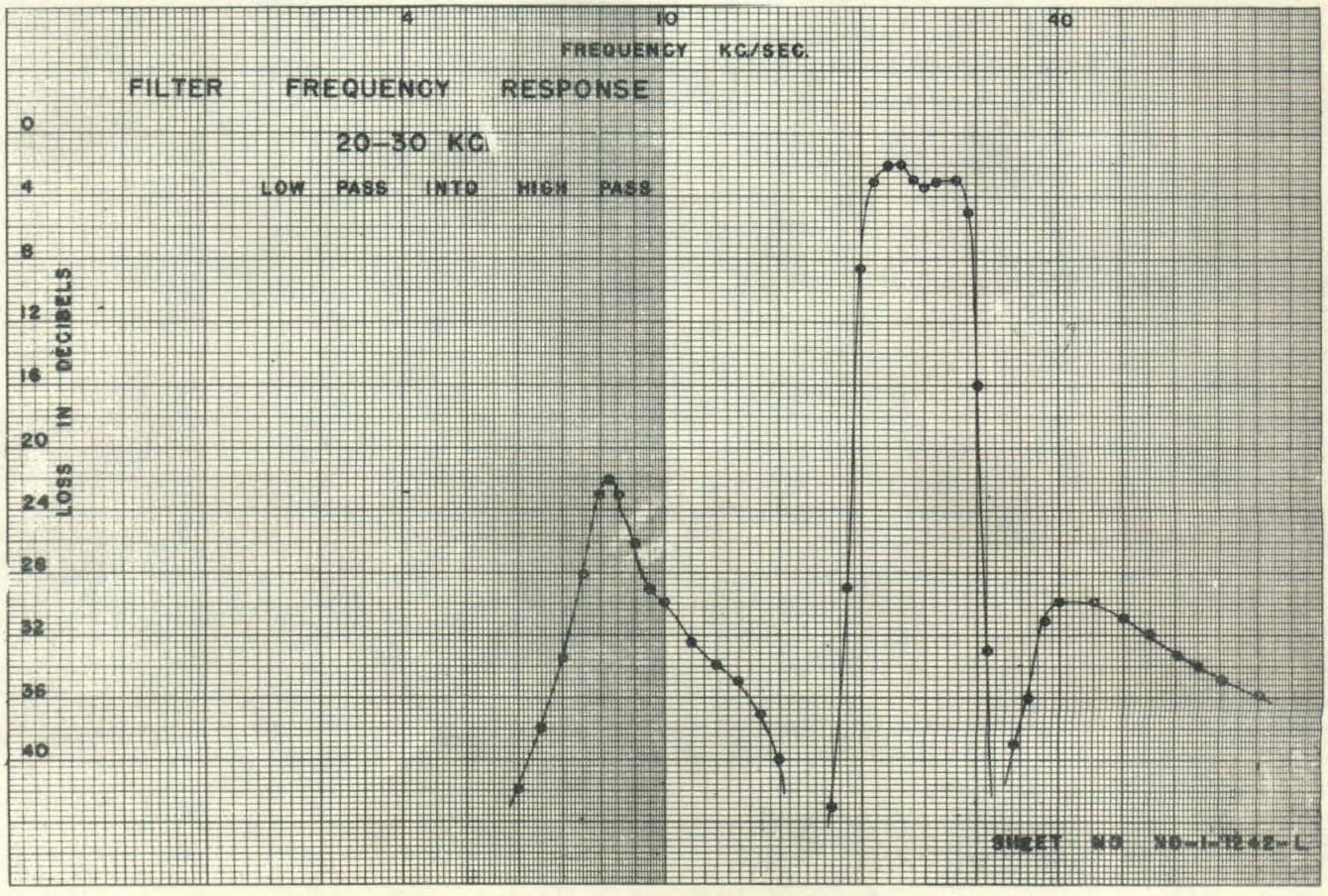
4
10
40
FREQUENCY KC/SEC.
FILTER FREQUENCY RESPONSE
20-30 KC.
LOW PASS INTO HIGH PASS
0
4
8
12
16
20
24
28
32
36
40
LOSS IN DECIBELS
SHEET NO ND-1-1242-L

FIG. A—14

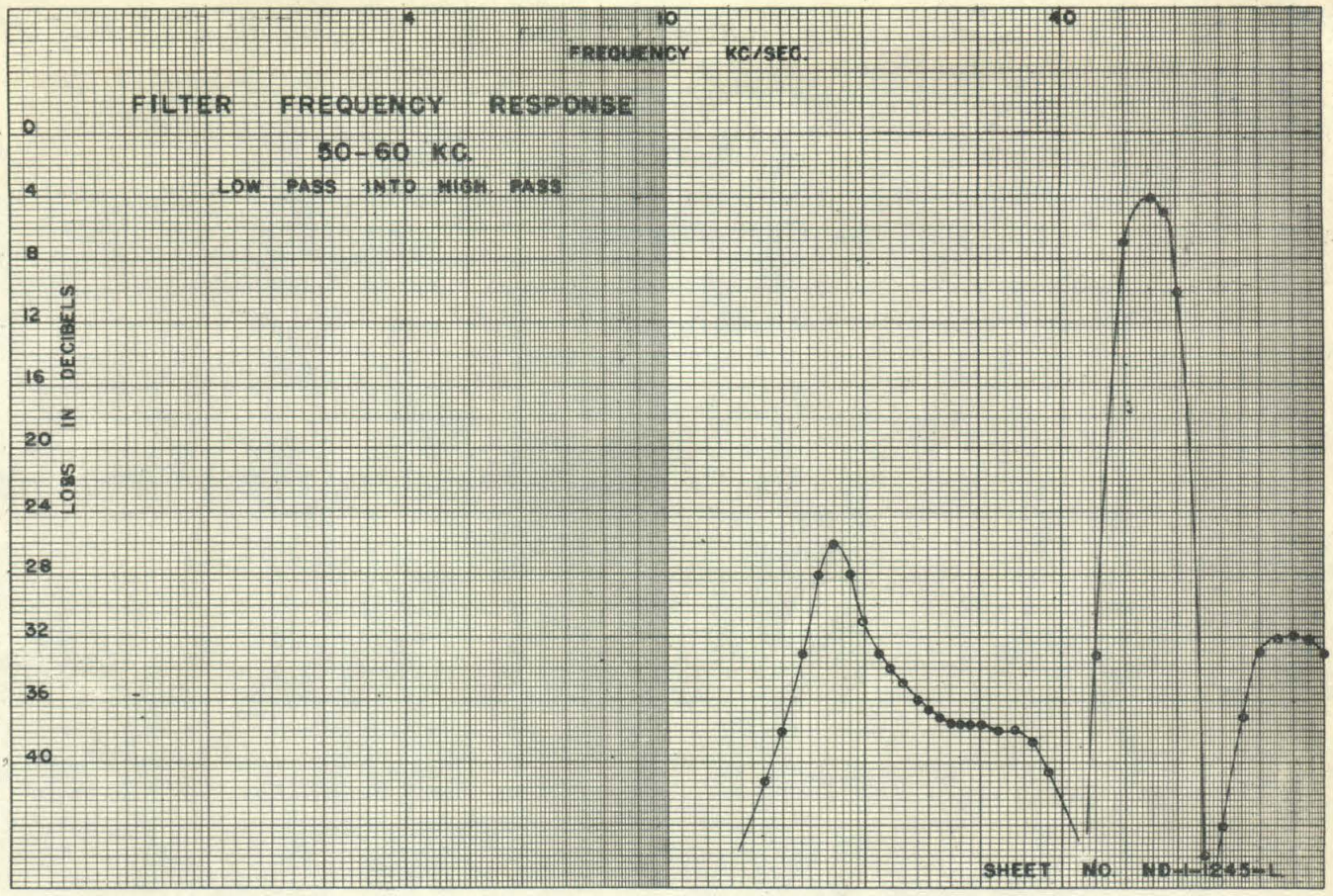
4
10
40
FREQUENCY KC/SEC.
FILTER FREQUENCY RESPONSE
50-60 KC.
LOW PASS INTO HIGH PASS
0
4
8
12
16
20
24
28
32
36
40
LOSS IN DECIBELS
SHEET NO. ND-1-1245-L

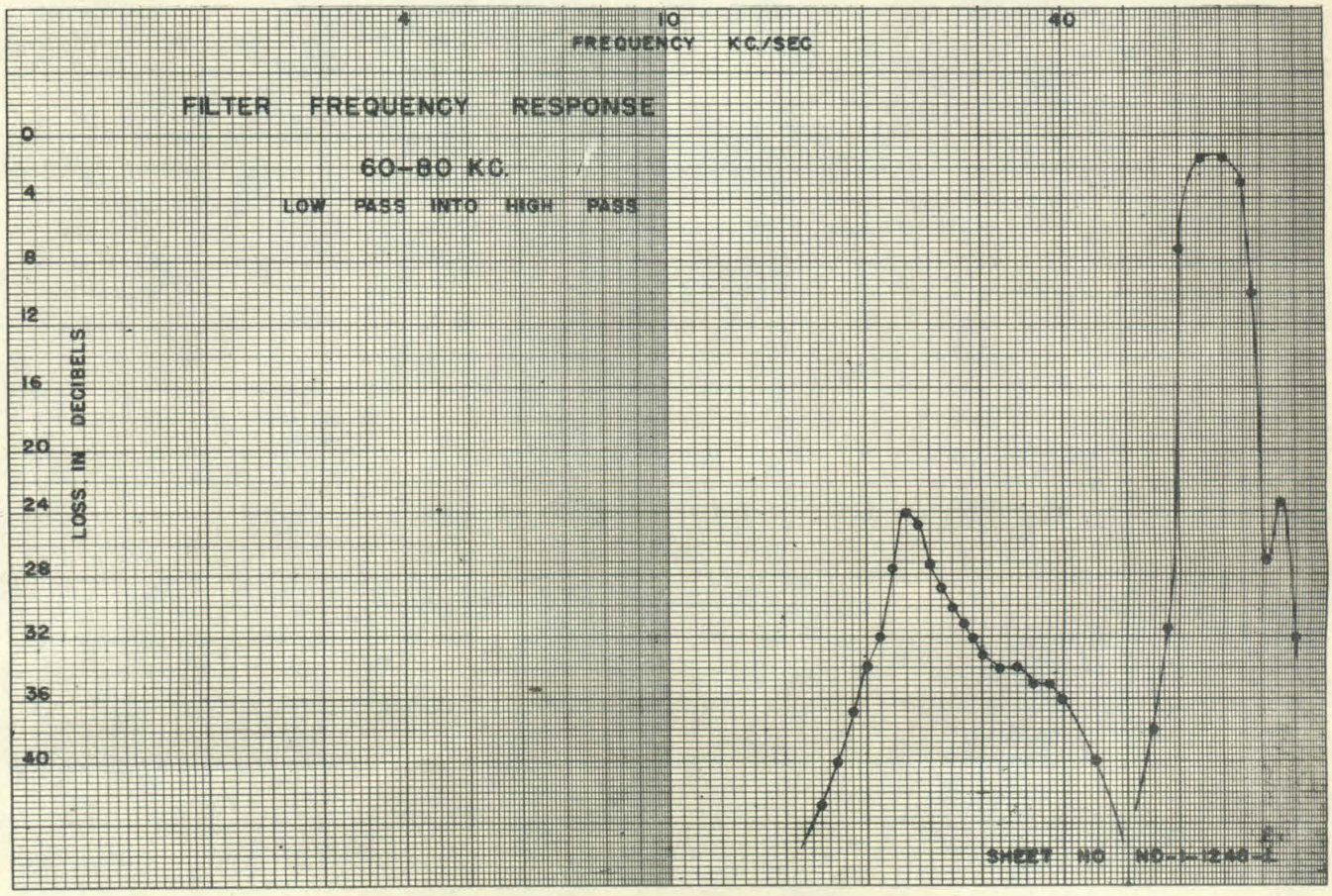
4
10
40
FREQUENCY KC./SEC
FILTER FREQUENCY RESPONSE
60-80 KC.
LOW PASS INTO HIGH PASS
0
4
8
12
16
20
24
28
32
36
40
LOSS IN DECIBELS
SHEET NO ND-1-1246-L

FIG. A-16

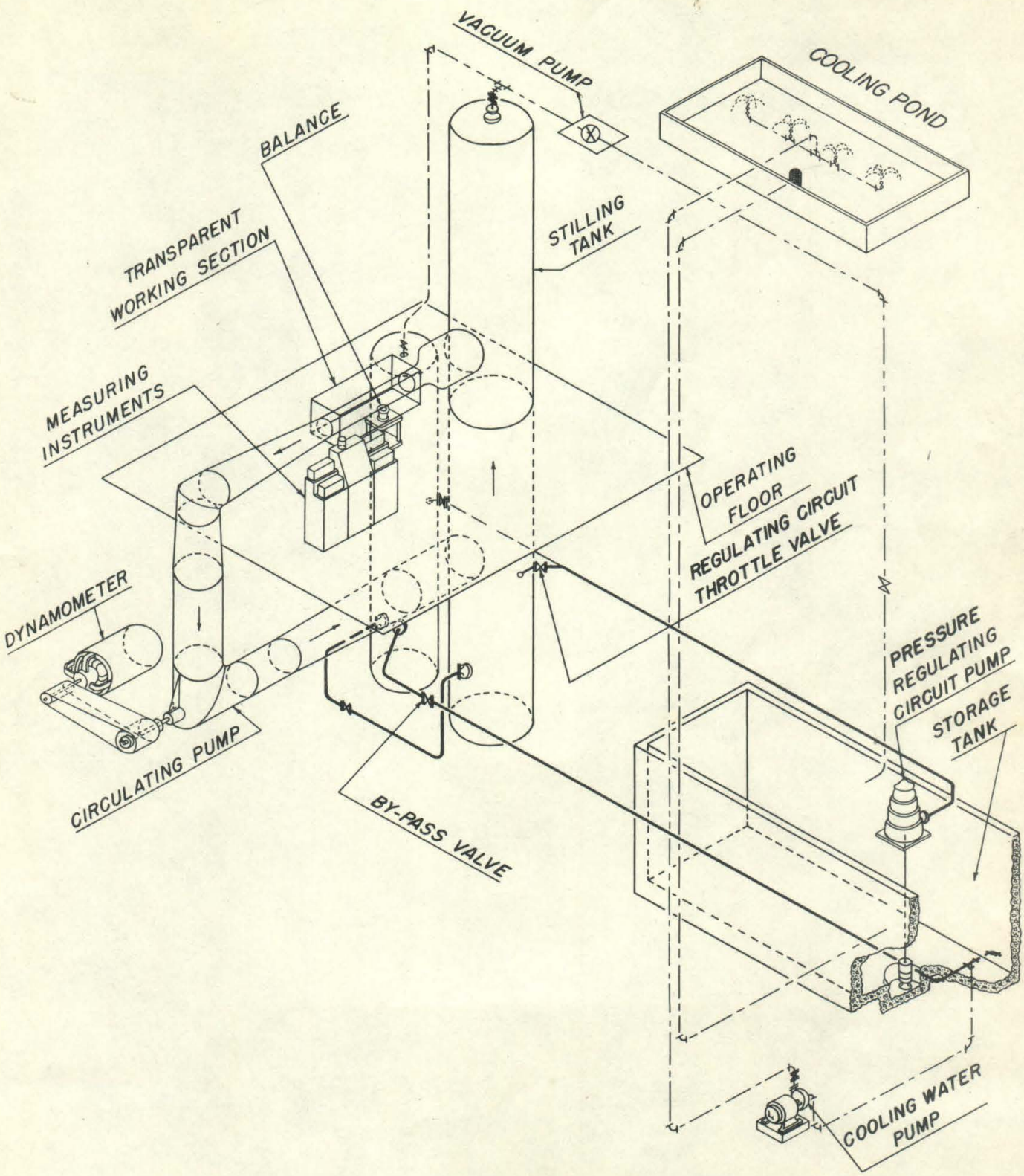
VACUUM PUMP
COOLING POND
BALANCE
TRANSPARENT WORKING SECTION
STILLING TANK
MEASURING INSTRUMENTS
OPERATING FLOOR
REGULATING CIRCUIT THROTTLE VALVE
DYNAMOMETER
PRESSURE REGULATING CIRCUIT PUMP
STORAGE TANK
CIRCULATING PUMP
BY-PASS VALVE
COOLING WATER PUMP

FIG. A-18

V. REFERENCES:

(1) For a complete description of the High Speed Water Tunnel and the construction of the models used for these experiments, see "The High Speed Water Tunnel at the California Institute of Technology", by R. T. Knapp, V. A. Vanoni, and J.W. Daily, HML Report No. ND1, June 29, 1942.

(2) "Water Tunnel Tests of a Model of a 14 Foot Torpedo", by R. T. Knapp. HML Report No. ND 8.3 (In preparation).